Pro-Opiomelanocortin (POMC) neurons in the nucleus of the solitary tract mediate endorphinergic endogenous analgesia in mice

Pro-Opiomelanocortin (POMC) neurons in the nucleus of the solitary tract mediate endorphinergic endogenous analgesia in mice.

Pabitra Hriday Patra[1], Becks Tench[1], Timna Hitrec[1], Fiona Holmes[1], Robert Drake[1], Serena Cerritelli[2], David Spanswick[3], and Anthony Edward Pickering[1]

1 - Anaesthesia, Pain & Critical Care Research, School of Physiology, Pharmacology and Neuroscience, University of Bristol, BS8 1TD, UK

2 – Radcliffe Department of Medicine, University of Oxford, John Radcliffe Hospital, Oxford, OX3 9DU, UK

3 - Neurosolutions, University of Warwick, Gibbet Hill Road, Coventry, West Midlands, CV4 7AL, UK

Corresponding Author AEP –Tel: +44 (0)1173312311 E-mail: Tony.Pickering@bristol.ac.uk.

Abstract

The nucleus of the solitary tract (NTS) contains pro-opiomelanocortin (POMC) neurons which are one of the two major sources of β-endorphin in the brain. The functional role of these NTS_{POMC} neurons in nociceptive and cardiorespiratory function is debated. We have shown that NTS_{POMC} optogenetic activation produces bradycardia and transient apnoea in a working heart brainstem preparation and chemogenetic activation with an engineered ion channel (PSAM) produced opioidergic analgesia *in vivo*. To better define the role of the NTS_{POMC} neurons in behaving animals, we adopted *in vivo* optogenetics (ChrimsonR) and excitatory/inhibitory chemogenetic DREADD (hM3Dq/hM4Di) strategies in POMC-Cre mice. We show that optogenetic activation of NTS_{POMC} neurons produces time-locked, graded, transient bradycardia and bradypnoea in anaesthetised mice which is naloxone sensitive (1 mg/kg, i.p) suggesting a role of β-endorphin. Both optogenetic and chemogenetic activation of NTS_{POMC} neurons produces sustained thermal analgesia in behaving mice which can be blocked by naloxone. It also produced analgesia in inflammatory pain (carrageenan) but not in a neuropathic pain model (tibial nerve transection). Inhibiting NTS_{POMC} neurons does not produce any effect on basal nociception but inhibits stress-induced analgesia (unlike inhibition of arcuate POMC neurons). Activation of NTS_{POMC} neuronal populations in conscious mice did not cause respiratory depression, anxiety or locomotor deficit (in open field) nor affective preference. These findings indicate that NTS_{POMC} neurons play a key role in the generation of endorphinergic endogenous analgesia and can also regulate cardiorespiratory function.

Key words: β-endorphin, pro-opiomelanocortin, nucleus of the solitary tract, analgesia, bradycardia, bradypnoea, optogenetics, DREADD chemogenetics

1 Introduction

Pro-opiomelanocortin (POMC) is the precursor of several important neuroactive peptides including β-endorphin, α-melanocyte-stimulating hormone (α-MSH) and adrenocorticotrophic hormone (ACTH)[7]. Within the brain, POMC neurons are concentrated in only two regions: the arcuate nucleus of the hypothalamus (ARC) and the nucleus of the solitary tract (NTS) of the medulla[3;6;53]. In the mouse there are approximately 3000 POMC neurons in the ARC, whereas the NTS contains 200-300 POMC neurons[24]. Multiple studies have reported a prominent role of ARC_{POMC} neurons in long term regulation of feeding behaviour and energy homeostasis mediated by α-MSH[3;6;53]. In contrast, NTS_{POMC} neurons have been shown to have a short term role in the regulation of feeding[13;57].

POMC neurons are also implicated in the regulation of nociception by the production of β-endorphin[7;47], an endogenous opioid peptide that acts with high affinity at μ-opioid receptors[15;34]. β-endorphin has been linked to the *'opioid burn'* analgesia of exercise[9;12;37;44] and it is causally involved in the mediation of stress-induced analgesia[47]. In addition to its role in analgesia, β-endorphin is also reported to be involved in reward processing[51], sexual behaviour[4] and cardiorespiratory control[31].

Although this evidence indicates that central β-endorphin has roles in the mediation of endogenous analgesia and cardiorespiratory control, the circuit mediation of these roles is less clearly defined. More attention has focussed on the hypothalamic ARC_{POMC} neurons and the involvement of NTS_{POMC} neurons in these actions is still debated. We previously demonstrated that chemogenetic activation of POMC neurons (using the pharmacologically selective actuator module (PSAM) strategy[32]) produces analgesia *in vivo* in the tail-flick assay[13]. We also showed that optogenetic activation of NTS_{POMC} neurons produces marked bradycardia and bradypnoea in the working heart brainstem preparation[13]. These cardiorespiratory depressant effects were produced by short synchronous bursts of optoactivation in a decerebrate preparation. Thus, it was unclear how more physiological modulation of activity of the NTS_{POMC} neurons would play in the regulation of heart rate and respiration *in vivo.* Such cardiorespiratory depressant actions could compromise the potential analgesic utility of their selective activation.

In an initial pilot investigation using assays of respiration to address this question we found that the chemogenetic ligand $PSEM^{89S}$ (90mg/kg), also had effects in control mice. We therefore designed the present study employing excitatory optogenetics[56] as well as

DREADD-mediated chemogenetics[46] to test whether NTS_{POMC} neuronal activation in mice *in vivo* is analgesic in acute, inflammatory and neuropathic pain models and/or has cardio-respiratory depressant effects. We extended our study to assess the role of these neurons in mediating stress-induced analgesia employing an inhibitory DREADD-mediated subtractive chemogenetic strategy.

2 Materials and methods

All procedures followed the UK Animals (Scientific Procedures) Act of 1986 and were approved by the University of Bristol Animal Welfare and Ethical Review Board.

2.1 Animals

Experiments were conducted on adult male and female transgenic POMC-Cre mice[5] bred and housed in the animal facility at the University of Bristol. All mice were maintained in 12h:12h light:dark cycle, a room temperature of 20±1˚C and humidity of 50±10%, with ad libitum access to food and water. We did not have any sex-specific hypotheses for the study and both male and female mice were randomly allocated to experimental groups. The surgical procedures, viral vector injections and behavioural testing conducted on each group of mice is detailed in Supplementary Table 1.

2.2 Viral vectors

The following adeno-associated viral vectors (AAV) were used in the study to express opto- and chemo-genetic actuators in POMC neurons.

AAV-ChrimsonR-tdTomato[28] (AAV-Syn-FLEX-rc[ChrimsonR-tdTomato], gift from Edward Boyden, serotype AAV5; titre 1.1×10^{13} GC/ml; Addgene vector prep #62723, USA) microinjected in the NTS for optogenetic experiments producing **$NTS_{POMC(Chrim)}$** mice.

AAV-hM3Dq-mCherry[29] (AAV-hSyn-DIO-hM3D(Gq)-mCherry, gift from Bryan Roth, serotype AAV2, titre 2×10^{13} GC/ml, Addgene USA, viral prep # 44361-AAV2) microinjected for excitatory chemogenetic experiments producing **$NTS_{POMC(Gq)}$** mice.

AAV-hM4Di-mCherry (rAAV2/hsyn-DIO-hM4D(GI)-mCherry, titre 4.6×10^{12} GC/ml, Addgene USA) was microinjected to the NTS or ARC for inhibitory chemogenetic experiments producing **$NTS_{POMC(Gi)}$** and **$ARC_{POMC(Gi)}$** mice (respectively).

AAV-hSyn-FLEX-PSAM-5HT$_3$ (stock viral titre $2.8\text{x}10^{12}$ GC/ml, diluted 1:10 with sterile PBS; Scott Sternson, Janelia Research Campus, VA, USA) was microinjected into the NTS of POMC-Cre mice[13] producing **$NTS_{POMC(PSAM)}$** mice.

AAV-EF1α-DIO-ChR2-mCherry (UNC Vector Core Services, Chapel Hill, NC; $6\text{x}10^{12}$ viral particles/ml) was injected for control experiments for the PSAM spirometry experiments.

2.3 Viral vector injection and optic fibre implantation

Recovery surgery for vector injection was performed under general anaesthesia with ketamine (70mg/kg, i.p) and medetomidine (0.5mg/kg, i.p). Two approaches were taken for viral vector injections which yielded similar patterns of transduction.

For the majority of studies the viral vector was injected into the medulla via the atlanto-occipital foramen as per Cerritelli *et al*.[13]. In brief, the mouse was positioned in a stereotaxic frame with its head angled down 20˚ from the horizontal. A small midline skin incision was made from the occiput down over the neck. The neck muscles were parted to reveal the atlanto-occipital membrane which was incised to get a view of area postrema. Calamus scriptorius, located on the dorsal surface of the medulla, was used as the reference for the stereotaxic injections. A vector-filled pulled glass pipette was placed at the rostro-caudal level of the tip of calamus scriptorius, 0.2 mm lateral to the midline and at a 35° angle to the vertical. Vector injections (180 nl over 2 min) were made unilaterally at 4 sites (0.25, 0.50, 0.75 and 1.00 mm) below the surface of the medulla.

For the chronically implanted optogenetic studies in behaving mice a trans-cerebellar approach was used for the NTS vector injections as this provided a better skull anchorage for the optic fibre. The anaesthetised mouse was placed in the stereotaxic frame with the skull level and a 1 mm diameter burr hole was made (-7.5 mm AP and 0.2 mm ML from bregma). The AAV was injected at four sites along a vertical track (180 nl at each site located 3.25, 3.5, 3.75 and 4 mm below the cerebellar surface). The optic fibre was implanted during the surgery at the same co-ordinates to a depth of 4 mm below the cerebellar surface (Lambda-B fibre 0.66NA, 200µm core diameter, emitting length 2 mm, implant length = 5 mm; Optogenix, Italy). These optical fibre implants are advantageous because of the emission along the length of the taper as well as from the tip which illuminates a large volume of tissue *in vivo*[42]. Additionally the large numerical aperture (0.66) efficiently collects the light from the LED and its penetration into the tissue is enhanced by the longer wavelength of light (620nM) used for activation of the red-shifted excitation spectrum of the optimised opsin ChrimsonR[28] compared to ChannelRhodopsin2. A stainless-steel anchoring screw was implanted over the occiput and the fibre was fixed with dental cement (Dental Reline, UK).

For the hypothalamic ARC injections, anaesthetised mice were placed in a stereotaxic frame, the skull was levelled, the cranial surface exposed and two 1 mm diameter burr holes were made (-1.5 mm AP and ±1 mm ML from bregma). The injecting micropipette was angled

10° towards the midline and the appropriate AAV was injected at four sites along a vertical track (180 nl at 5.6, 5.8. 6.0 and 6.2 mm below the cerebellar surface).

Once the injection / implantation was completed the skin edges were sutured closed, and antiseptic wound powder was applied. Mice were given atipamezole (1 mg/kg, i.p) to reverse the anaesthesia and buprenorphine (0.1 mg/kg, s.c.) for analgesia. All experiments were conducted at least 3 weeks after AVV injection.

2.4 Acute medullary slice electrophysiology

At 3-5 weeks post AAV injection, the $NTS_{POMC(Chrim)}$ mice were terminally anaesthetised using isoflurane (5%), then decapitated. The brainstem was dissected free and submerged in ice-cold, carbogenated, slicing artificial cerebrospinal fluid (ACSF) containing (mM): 26 $NaHCO_3$, 1.2 KH_2PO_4, 1.9 KCl, 0.4 $CaCl_2$, 3.9 $MgCl_2$, 10 glucose, 154 sucrose and 0.34 ascorbic acid. Coronal slices of medulla were cut in the ventral to dorsal direction (300 μm thick). Slices rested at 34°C for 30 minutes in cutting solution before being transferred to recording ACSF of the same temperature for a further 30 minutes before being kept at 20˚C. Recording ACSF contained (mM); 126 NaCl, 26 $NaHCO_3$, 1.25 NaH_2PO_4, 2.5 KCl, 2 $CaCl_2$, 2 $MgCl_2$ and 10 glucose at pH 7.3.

Visualised patch clamp recordings were obtained from slices in a heated bath (34°C) perfused with ACSF at 2.5 ml/min on the stage of a Leica DMLFSA microscope. Neuronal profiles were visualised with Dodt gradient contrast. Epifluorescence illumination from a mercury light source via filter cube (N2.1, excitation filter 515-560 nm) was used to visualise the tdTomato in labelled neurons and axonal projections within the slice (Figure 1A). Patch pipettes were pulled from thin wall filamented glass (Harvard Apparatus GC120F-10). They were filled with internal solution containing (mM): 130 K-gluconate, 10 KCl, 10 Na-HEPES, 0.2 EGTA, 4 MgATP and 0.3 Na_2GTP, pH 7.3 and 310 mOsm. Filled pipettes had a tip resistance of 6-9 MΩ. Illumination for optogenetic activation was delivered from a 620nm LED (11mW PlexBright module, Plexon) coupled to a 200 μm diameter optic fibre placed above the target cells.

Current / voltage clamp recordings were made with a Multiclamp 700A patch amplifier (Axon Instruments) controlled by Multiclamp 700A commander software. Data was low pass filtered at 3kHz before being sampled at 10kHz (Micro 1401, Cambridge Electronic Design), to enable acquisition in Spike (v7) or Signal (v5). WinWCP (V5.2.0) (John Dempster,

University of Strathclyde, UK) was used for analysis of photocurrents. Figures created in Inkscape (v0.48), ImageJ (v1.51) and OriginPro (v2018b).

2.5 Cardiorespiratory recordings in vivo

2.5.1 Acute optogenetic activation of NTS_{POMC} neurons in anaesthetised mice

ECG and thoracic respiratory muscle EMG were recorded under anaesthesia (urethane 0.8g/kg, i.p, n=3 mice) to assess the effect of opto-stimulation on heart rate and respiration (respectively) in $NTS_{POMC(Chrim)}$ mice. Needle electrodes (23-gauge) were inserted subcutaneously into the animal over the chest. The electrodes were connected to custom-built AC amplifier (x5-10K, PPN electronic workshop, University of Bristol). Instantaneous heart rate was monitored using a window discriminator to trigger off the R wave of the ECG signal. All signals were acquired with an analogue to digital converter (micro1401, CED, Cambridge, UK) to a computer running Spike2 software (CED). Intercostal EMG was extracted from the same recording by rectifying the signal and applying a median filter (time constant 60ms) in Spike2 to monitor respiratory pattern.

For these acute optogenetic experiments, a 200µm optic fibre (Lambda-B fibre, emitting length 2mm + implant length 17mm; Optogenix, USA) connected to 550 nm LED (Lime PlexBright module, Plexon, USA) was inserted 0.25 mm into the NTS from the surface of the medulla at the level of *calamus scriptorius*. The NTS was illuminated with 20ms light pulses at 5-20 Hz for 5s (2-3 min interval between consecutive stimulus trains). Three repetitions of each light train were applied at each frequency. The light intensity exiting the fibre was ~6mW (measured before and after each experiment, Thorlabs power meter, PM400D). These were proof-of-concept experiments which informed the approach employed for the optogenetic experiments in chronically implanted mice (described below).

2.5.2 Chronic implanted optogenetic activation of NTS_{POMC} neurons

$NTS_{POMC(Chrim)}$ mice with a previously implanted optic fibre had ECG and intercostal muscle EMG recorded under light, recovery, anaesthesia using isoflurane (maintenance isoflurane 1-1.5% in O_2). The anaesthetised mice were placed prone on a thermal heat pad. A wireless LED head-stage (Helios 620 nm, Plexon Inc, USA) was connected to the fibre optic. The light intensity exiting the fibre was ~2mW (measured at implantation). The ECG/EMG recording arrangement was as for the acute ECG/EMG study (see 2.5.1) except that the signal was amplified and digitised using an INTAN head-stage (RHD2216) and the digitised signal was relayed via an acquisition system (Open-Ephys.org). The data was displayed and analysed

in Spike2 and cardiorespiratory responses elicited using identical light stimulation parameters to those from the acute experiments. The involvement of endogenous opioids in the optogenetically-evoked (20ms×20Hz, 5s) cardiorespiratory responses was assessed 30 min after injection of either the opioid antagonist naloxone (1 mg/kg, i.p) or 0.9% normal saline (NSS; i.p). The experimenter was masked to drug identity with testing on different days (counterbalanced design). The experiment was also conducted in control implanted $NTS_{POMC(Gq)}$ mice (n=4) to test whether an identical pattern of light stimulation alters cardiorespiratory function in mice without ChrimsonR expression.

2.5.3 Analysis of ECG and EMG data

Instantaneous heart rate was calculated from the reciprocal of the R-R interval of ECG. The inter-breath interval was calculated from onset of bursts in the intercostal EMG. To analyse the effect of opto-stimulation the recording was divided into four phases: pre-basal (***P***, 10s), baseline (***B***, 10s), during opto-stimulation (***O***, 5s) and recovery (***R***, 10s) (shown in Supplemental Figure 1). The degree of bradycardia (%) was calculated (taking account of the spontaneous variation in heart rate and respiration within each of these periods) from the heart rate (HR) using the following formulae:

Baseline bradycardia (%) = (mean ***P*** – minimum ***B***)/mean ***P*** × 100

Opto-stimulation bradycardia (%) = (mean ***P*** – minimum ***O***)/mean ***P*** × 100

Recovery bradycardia (%) = (mean ***P*** – minimum ***R***)/mean ***P*** × 100

Similarly, the degree of bradypnoea (%) was calculated from the maximum inter-breath intervals using the following formulae:

Baseline bradypnoea (%) = (maximum ***B*** – mean ***P***)/mean ***P*** × 100

Opto-stimulation bradypnoea (%) = (maximum ***O*** – mean ***P***)/mean ***P*** × 100

Recovery bradypnoea (%) = (maximum ***R*** – mean ***P***)/mean ***P*** × 100.

To derive the opto-stimulation Δbradycardia (%) the baseline bradycardia (%) was subtracted from the opto-stimulation bradycardia (%). Similarly, Δbradypnoea (%) was derived from the difference between baseline bradypnoea (%) and opto-stimulation bradypnoea (%).

2.6 Acute pain assays

2.6.1 Hargreaves' test

Hargreaves' test was conducted to assess the degree and time-course of analgesia[20]. In this test, a beam of infrared light (Harvard Apparatus, USA) was directed onto the plantar surface of the hind paw and the withdrawal latency was recorded. A fixed intensity of

illumination that produced a withdrawal latency between 3-5 seconds (for optogenetics and excitatory chemogenetics) or 5-7 seconds (for inhibitory chemogenetics) under baseline conditions was determined prior to the test session and used throughout the experiments. A maximum cut-off latency for the Hargreaves' test of 15 s was employed to avoid tissue injury. All mice were habituated to the test apparatus for 3 days prior to experiment.

Implanted $NTS_{POMC(Chrim)}$ mice received opto-stimulation using the wireless LED headset (20 ms pulses x 5 Hz, 1 min) to assess the effect on thermal withdrawal. To establish the time-course of any effect the mice had a single period of opto-stimulation and the withdrawal latency was assessed over the next hour (at 5, 10, 20, 30, 40, 50 and 60 min). Each $NTS_{POMC(Chrim)}$ (n=6) mouse was then tested for three consecutive days (randomly allocated, counterbalanced design) under three conditions: i) baseline (without opto-stimulation) ii) opto-stimulation (20 ms pulses × 5 Hz, 1 min) after 0.9% normal saline solution injection (NSS, i.p) and iii) opto-stimulation after naloxone injection (1 mg/kg, i.p). Four repeated measures were taken under each condition at intervals of 10 min. Naloxone/NSS was administered 15 min before the start of first test. The experimenter was masked to drug (NSS/Naloxone). The same experimental protocol was repeated in control mice (implanted $NTS_{POMC(Gq)}$, n=6) to assess the effect of light alone on withdrawal latency in the Hargreaves' test.

The Hargreaves' test was also conducted for chemogenetic studies in $NTS_{POMC(Gq)}$ (n=6, excitatory) and $NTS_{POMC(Gi)}$ (n=6, inhibitory) mice. On different days the mice received either: i) NSS injection (i.p) or ii) Clozapine N-Oxide dihydrochloride injection (3 mg/kg, i.p, subsequently abbreviated to CNO). The $NTS_{POMC(Gq)}$ mice also had a third condition with naloxone (1 mg/kg, i.p) in addition to CNO injection. All drugs (NSS/CNO/Naloxone; i.p) were administered 15 min before the start of the first Hargreaves test and four repeated measurements were taken in each animal at intervals of 10 min. The experimenter was masked to drug allocation and the allocation to drug was counterbalanced. The experiment was also repeated with CNO dosing to control mice ($NTS_{POMC(Chrim)}$, n=6) to test whether CNO injection has an effect on withdrawal latency in Hargreaves' test.

2.6.2 Tail-flick test

The tail-flick test was conducted to assess the analgesic efficacy of activation of POMC neurons both by optogenetics and chemogenetics. The mouse was wrapped in a soft towel and 2-3 cm of its tail tip was dipped into water (45°C for optogenetic study and 50°C for chemogenetics) to assess the withdrawal latency. A cut-off of 20s for the tail flick was

employed to avoid tissue injury. The experimental comparisons were similar to the Hargreaves' test. The mice were habituated for 2 days before the test protocol. The experiment was also repeated in control vector injected mice (implanted $NTS_{POMC(Gq)}$, n=6 for optogenetics and $NTS_{POMC(Chrim)}$, n=6 for chemogenetics).

2.7 Conditioned place preference testing

Condition place preference (CPP) test was conducted in the $NTS_{POMC(Chrim)}$ (n=6) and $NTS_{POMC(Gq)}$ (n=6) mice to assess whether optogenetic or chemogenetic activation of NTS_{POMC} neurons respectively produces preference or aversion. The CPP testing apparatus consists of two distinct chambers (each 190x230mm, one with horizontal black and white striped walls and horizontal grating floor, and the other with vertical black and white striped walls and perforated floor. The chambers were joined by a clear plastic external corridor. Each animal was habituated for 15 min the day before the start of the conditioning protocol where the animal was allowed to freely explore both the chambers of the CPP box.

Each $NTS_{POMC(Chrim)}$ mouse was conditioned for two consecutive days (morning/afternoon) with opto-stimulation (20ms pulses at 5Hz for 5 min) in one of the CPP arena chambers (counter-balanced design). On the alternate session (morning/afternoon) of these two days the test animal was also allowed to freely explore the other chamber (non-conditioned) for 5 min with its head-stage attached. On the test day, the animal was placed inside the common external corridor between the two chambers (with the wireless LED head-stage attached) and allowed to freely explore the two chambers for 15 min.

For the chemogenetic experiments, each $NTS_{POMC(Gq)}$ mouse was allowed to spend 15 min/day either in the conditioned (CNO, 3 mg/kg, i.p, alternate days) or non-conditioned (NSS, i.p, alternate days) CPP chamber for four days. During this conditioning phase the animals were dosed with CNO / NSS and then returned to their home cage for 15 minutes before being put in the CPP chamber. On the test day, the animal was placed inside the common external corridor between the two chambers and allowed to freely explore the two chambers for 15 min.

The experiments were video-recorded, and the video files were coded allowing blinding before analysis. The time spent in each chamber before (15 min habituation period) and after conditioning (15 min test period) was analysed (Ethovision, Noldus, Netherlands). The proportion of time spent by the animals between conditioned and unconditioned chamber was compared. Additionally, the percentage of time spent in the conditioned chamber by each animal before and after conditioning was also contrasted.

2.8 Open field test

Open field testing was conducted to determine whether chemogenetic activation of NTS_{POMC} neurons caused any anxiolytic changes in behaviour or locomotor activity in the $NTS_{POMC(Gq)}$ mice (n=5). In this test, 15 min after the injection of CNO (3 mg/kg, i.p) the mouse was placed in an open field box (50×50 cm) and allowed to freely move around the arena for 15 min. The experiment was also conducted in control mice ($NTS_{POMC(Chrim)}$, n=4) employing the same protocol for comparisons. The test was video recorded and blinded off-line analysis was done to evaluate the time spent in the central arena and the total distance moved by the experimental vs control mice.

2.9 Persistent pain models

2.9.1 Tibial nerve transection

To produce a neuropathic pain model, mice underwent surgery for tibial nerve transection (TNT), a model that has shown to induce robust and long-lasting hypersensitivity[22;23;30;45]. Mice were anaesthetized with isoflurane (5% in O_2 until loss of consciousness and maintained at 1-2% isoflurane in O_2). A 5 mm incision was made through the skin over the right thigh parallel to the femur and the sciatic nerve was exposed allowing identification of the tibial nerve. The isolated tibial nerve branch was ligated with 6-0 silk thread as distally as possible. 3 mm of the nerve proximal to the ligation was transected and removed, and the ligature was left in place. The skin was sutured with 6-0 silk thread and the animals were left to recover for 1 week. Sensory testing with acetone (cold sensitivity) and von Frey filaments (punctate pressure sensitivity) was undertaken before surgery and again 2 - 3 weeks following nerve transection after administration of CNO / NSS.

2.9.2 Carrageenan inflammatory pain model

Inflammatory sensitisation was induced by injecting the plant derived mucopolysaccharide, λ-carrageenan, following the protocol of McCarson and colleagues[33]. Mice were briefly anaesthetised with isoflurane and the right hind paw was disinfected with 70% ethanol and iodine solution. Then 25µl of 0.5% λ-carrageenan (Merck, dissolved in sterile dH_2O) was injected (25G syringe needle) in the right hind paw foot pad. Mice were returned to their cage and developed sensitisation and oedema after approximately 3.5 hours, which lasted until the end of the experiment (8 hours). Sensory testing (von Frey) was conducted 15 minutes after administration of NSS / CNO (administered sequentially with > 1 hour between i.p injections, at 3.5 and 5 hours post carrageenan respectively). A subsequent set of tests was

conducted 2.5 hours post-CNO injection to assess whether any effect of chemo-activation resolves by this time point.

2.9.3 Punctate mechanical - von Frey test

To assess the degree of mechanical hyperalgesia, animals that underwent either tibial nerve transection (n=6) or carrageenan injection (n=4) were tested by applying von Frey filaments of varying force in the mid-lateral plantar area of the right hind paw, to identify the threshold that produces a withdrawal. The starting filament applied was 1 g (4.08). The 50% withdrawal threshold was identified using the up and down method (Chaplan et al., 1993), and is reported in grams.

2.9.4 Cold sensitivity - Acetone test

To identify the presence of cold allodynia in TNT mice (n=6), a drop of acetone was applied to the mid-lateral plantar area of the right hind paw and the nocifensive events (paw raises, licking, shaking) were scored over 60 seconds. The test was repeated three times five minutes apart and the mean value is reported.

2.10 Spirometry

To assess whether activation of NTS_{POMC} neurons produces respiratory depression in freely behaving mice spirometry was conducted in plethysmography chambers (EMKA Technologies, France), supplied with room air, and with differential pressure transducers connected to a computer. All mice were habituated to the apparatus for 30 min the day before the experiment. The experiment was conducted on 2 consecutive days where each mouse (**$NTS_{POMC(PSAM)}$** or **$NTS_{POMC(Gq)}$**) respectively received either chemogenetic agonist ($PSEM^{89s}$ 90mg/kg) or CNO (3mg/kg, i.p) compared to control NSS (i.p) (counterbalanced design). The minute volume was recorded in the plethysmograph for 60 min under each condition. A 15 min baseline recording was taken before the start of the experiment. The experiment was also conducted in control mice ($NTS_{POMC(Chrim)}$, n=2) using the same test protocol. Drug administration was randomised, and the experimenter was blinded to the treatment.

Initial experiments using the PSAM strategy (Cerritelli et al 2016) showed evidence for a significant depression of respiration with $PSEM^{89s}$ when compared with NSS (Supplemental Figure 2) but a similar degree of respiratory depression was observed in control mice suggesting that this dose of $PSEM^{89s}$ had off target effects on respiratory control and so all subsequent experiments used the DREADD hM3Dq chemogenetic strategy.

2.11 Stress induced analgesia

A 3-min swim in 32°C water[14;47] was used to generate stress-induced analgesia. This was assessed with tail-flick assay performed before and 1 min after the swim. For the tail-flick assay the mouse was dried and wrapped with a soft towel and the distal third of its tail was dipped into 50°C water to measure the tail withdrawal latency. Both the $NTS_{POMC(Gi)}$ (n=8) / $ARC_{POMC(Gi)}$ (n=3) and control ($NTS_{POMC(Chrim)}$, n=6) mice were injected with either CNO or NSS 15 min prior to the swim which was repeated on consecutive days (counterbalanced design, experimenter blinded to drug). Two repeat measurements (at 1 min intervals) were taken at each time point to obtain the average tail withdrawal latency.

2.12 Histology

All mice were euthanised (pentobarbital sodium 100mg/kg, i.p) at the end of study and brains were fixed by cardiac perfusion with 10% formalin. Following fixation, the brains were post-fixed in 10% formalin for a day and then cryopreserved in 30% sucrose at 4˚C. Coronal slices (50µm) were cut on a freezing microtome, mounted and observed on an epifluorescent microscope (Leica DM4000B, Leica Microsystems, Wetzlar, GmbH) to confirm the expression of ChrimsonR-tdTomato/hM3Dq-mCherry/hM4Di-mCherry in the NTS/ARC. Animals that had failed virus transduction were excluded from the group and used as internal experimental controls as appropriate.

2.13 Statistical analysis

Statistical analysis was conducted using GraphPad Prism 7 (GraphPad Software, Inc., USA). Technical replicates obtained from each animal were averaged first before performing analysis. The statistical tests used for analysis are reported in the respective result sections. Results reported as mean ±SEM or median [IQR] as appropriate. Differences were considered significant at $P<0.05$ and experimental group sizes were based on the effect sizes from our previous study[13]. Where previous experimental data was not available then an initial pilot was conducted with n=3 animals to get an estimate of effect size and a power calculation was performed (beta<0.1 and alpha<0.05) to calculate the required group size. In most cases (unless otherwise specified) comparisons were made within animal (before vs after treatment). Experiments on control animals were done using the same testing protocol to demonstrate that observed effect was due to the optogenetic/chemogenetic modulation of the POMC neurons.

2.14 Materials

Naloxone hydrochloride (made to a stock solution of 10 mg/ml in dH_2O) and CNO dihydrochloride were from Tocris (Bristol, UK). All other salts and drugs were from Sigma unless otherwise stated.

3 Results

3.1 Opto-stimulation of NTS_{POMC} neurons in brain slices

To enable opto-stimulation of NTS_{POMC} neurons we aimed to express ChrimsonR which has the potential advantage in vivo of relatively large photocurrents and has a red shifted excitation spectrum which allows better light penetration in brain tissue[28]. To confirm the efficacy of optoexcitation, whole-cell recordings were made from NTS_{POMC} neurons transduced with ChrimsonR, identified by tdTomato fluorescence, in acute slices of medulla (Figure 1A, n=7). All of the tdTomato$^+$ neurons showed time-locked inward currents in response to pulses of illumination (610nm, 5-100ms; voltage clamped at V_h=-60mV) with a mean inward current 248 ± 114 pA (Figure 1B, n=7). Current clamp recordings of the same $NTS_{POMC(Chrim)}$ neurons showed that opto-stimulation could reliably drive action potentials with a 1:1 ratio in neurons with either 5 ms or 20 ms pulses at frequencies between 1 and 20Hz (Figure 1C).

3.2 High frequency opto-stimulation of NTS_{POMC} neurons in anaesthetised mice evokes transient bradycardia and bradypnoea

As a proof of concept experiment we assessed whether opto-stimulation of NTS_{POMC} neurons transduced with ChrimsonR produced changes in heart rate and respiration *in vivo* analogous to the effects seen *in situ* in the working heart brainstem preparation[13]. An acutely placed fibre-optic probe was lowered into the NTS of isoflurane anaesthetised mice (Supplemental Figure 1A-C, n=3). Opto-stimulation at 20Hz induced a bradycardia (7.8% [1.7-23.6%] vs baseline 0.06% [0.06-0.4%]; p=0.03, Friedman test with Dunn's *post-hoc* test; Supplemental Figure 1D-E), but this was not seen at lower frequencies (2Hz, p=0.22 or 5Hz, p=0.22, Friedman test). The bradycardia produced by 20Hz opto-stimulation was transient and returned to the baseline within 10s (recovery 1.0% [0.6-3.4%] vs baseline; Dunn's *post-hoc* test, p=0.44; Supplemental Figure 1E).

This opto-stimulation of NTS_{POMC} neurons simultaneously produced a graded bradypnoea with an increased inter-breath interval at 20Hz (213% [172-545%] vs baseline 8.2% [8.1-9.5%]; p=0.03) and 10Hz (81% [53-231%] vs baseline 14% [8.6-16%]; p=0.03, Friedman test with Dunn's *post-hoc* test) but not at 5Hz (53% [18-62%] vs baseline 8.9% [7.9-10.9%]; p=0.2; Supplemental Figure 1F). As with the bradycardia these respiratory pauses were short-lived and recovered to baseline within 10 seconds of the end of opto-stimulation (Dunn's *post-hoc* test, p=0.44).

The cardiorespiratory depressant effects were specific to NTS_{POMC} neuronal activation as no effect was observed when the probe was placed lateral or rostral to the NTS. The pattern of bradycardia and bradypnoea were identical in character to those seen in the working heart–brainstem preparation in response to activation of NTS_{POMC} neurons[13] which confirmed successful optogenetic targeting and activation of NTS_{POMC} neurons *in vivo* with ChrimsonR.

3.3 Opto-stimulation of NTS_{POMC} neurons in implanted mice produces a graded, transient bradycardia and bradypnoea

To allow longitudinal studies and combined assays of cardiorespiratory function and pain-related behaviours, $NTS_{POMC(Chrim)}$ mice (n=6) were implanted chronically with an optic fibre (Figure 2A-D). Recordings under isoflurane anaesthesia showed opto-stimulation produced graded transient bradycardia (Figure 2E & Supplemental Figure 3) with a reduction in heart rate at 5-20 Hz frequencies ($p<0.01$, Friedman test with Dunn's *post-hoc* test) but not at 2Hz (Friedman test, $p=0.052$). An identical illumination protocol in implanted control $NTS_{POMC(Dq)}$ mice did not produce any effect on heart rate even at the maximum stimulus frequency (20Hz, n=4, Figure 2F, Supplemental Figure 3E). Opto-stimulation in $NTS_{POMC(Chrim)}$ mice (n=6) also produced graded bradypnoea with an increase in inter-breath interval at all frequencies ($p<0.01$, Friedman test with Dunn's *post-hoc* test, Figure 2G & Supplemental Figure 3). Again, an equivalent illumination protocol in implanted $NTS_{POMC(Dq)}$ control mice had no effect on respiration (20Hz, n=4, Figure 2H). Both the bradycardia and bradypnoea were frequency dependent (Friedman test, $p<0.0001$). The opto-stimulation-induced Δbradycardia was significantly larger at 10Hz ($p=0.04$) compared to 2Hz and at 20Hz compared to both 2Hz ($p=0.0003$) and 5Hz (Dunn's *post-hoc* test, $p=0.04$; Figure 2I). Similarly, the Δbradypnoea was significantly larger at 10Hz ($p=0.01$) and 20Hz ($p=0.002$) compared to 2Hz (Figure 2J). The heart rate and respiratory rate rapidly recovered after illumination stopped (recovery vs baseline $p>0.05$).

3.4 NTS_{POMC} bradycardia is opioid mediated.

Administration of the opioid antagonist naloxone (1mg/kg, i.p) 30 min prior to opto-stimulation (20Hz) attenuated the NTS_{POMC}-evoked bradycardia (naloxone 31% [11-59%] vs NSS 56% [38-67%]; $p=0.03$, Wilcoxon matched-pairs signed rank test, Supplemental Figure 4) but not the bradypnoea (naloxone 203% [73-314%] vs NSS 339% [163-390%]; $p=0.31$, Supplemental Figure 4).

3.5 Opto-stimulation of NTS_{POMC} neurons produces sustained opioid-mediated analgesia

To investigate whether opto-stimulation of NTS_{POMC} neurons produces analgesia the tail-flick assay was employed. Based on the findings from the cardiorespiratory study above, we used a light stimulation paradigm that was the lowest frequency that produced consistent physiological effects (20ms × 5Hz). Such opto-stimulation in implanted $NTS_{POMC(Chrim)}$ mice increased the tail-flick latency (from 5.9±0.3s baseline to 18.8±0.6s, RM one-way ANOVA with Tukey's *post-hoc* test, n=6, $p<0.0001$, Figure 3B). This was attenuated by naloxone treatment (9.33±0.85s vs 18.8±0.6s NSS, p=0.0004; 1mg/kg, i.p 15 min prior to test; Figure 3B) but this did not completely return the latency to baseline (Tukey's *post-hoc* test, p=0.01). Implanted control mice showed no change in their tail-flick latency after identical illumination (implanted $NTS_{POMC(Gq)}$, p=0.43, paired t-test, n=6, Figure 3C).

A similar analgesic action was also found in the Hargreaves' test. NTS_{POMC} opto-stimulation (20ms × 5Hz, 1min) increased hind paw withdrawal latency (RM one-way ANOVA, $p<0.0001$, n=6). This showed an increase in paw withdrawal latency following opto-stimulation (10.7±0.9s NSS vs 4.5±0.8s baseline, p=0.0005, Tukey's multiple comparison test Figure 3D). Naloxone attenuated the effect of NTS_{POMC} opto-stimulation on paw withdrawal latency (6.2±0.5s, Tukey's *post-hoc* test, p=0.002; 1 mg/kg, i.p inj. 15 min prior to test; Figure 3D) compared to NSS but there was still a small increase in withdrawal latency compared to baseline (Tukey's *post-hoc* test, p=0.02). No change in withdrawal latency was observed in implanted control mice following opto-stimulation (implanted $NTS_{POMC(Gq)}$, p=0.82, paired t-test, n=6, Figure 3E).

To determine the time course of analgesic effect, NTS_{POMC} neurons in the same implanted $NTS_{POMC(Chrim)}$ mice were opto-activated (for 1 min at 5Hz) and the hind paw withdrawal latency assessed repeatedly using the Hargreaves' test (Figure 3F). The withdrawal latency showed a significant effect of time (RM one-way ANOVA, $p<0.0001$, n=6). The withdrawal latency was prolonged during opto-stimulation (14.2±0.5s, $p<0.001$) and it remained elevated for the following 30 mins (5 min (9.5±0.8s, $p<0.01$), 10 min (8.9±0.7s, $p<0.001$), 20 min (8.2±0.7s, $p<0.001$) and 30 min (6.9±0.8s, $p<0.01$)) compared to baseline (4.9±0.7s).

3.6 Opto-stimulation of NTS_{POMC} neurons does not produce preference / aversion

Given that the naloxone blockade of the analgesic effects suggested the release of β-endorphin from NTS_{POMC} neurons we sought to identify whether this had an affective valence

in the CPP test. No difference was observed in the time spent by these implanted $NTS_{POMC(Chrim)}$ mice between the opto-stimulation conditioned vs unconditioned chamber (52.6±5.1% vs 47.4±5.1%, respectively, n=6, p=0.49, Welch's t-test; Figure 3G). Furthermore, the time spent in the conditioned chamber before (15 min habituation period) and after conditioning (15 min test period) was also unchanged (51.6±3.1 vs 52.6±5.1%, n=6, p=0.87, Welch's t-test, Figure 3H).

3.7 Chemogenetic activation of NTS_{POMC} neurons produces analgesia

The synchronous opto-activation of NTS_{POMC} neurons is likely to be a non-physiological pattern of activity and therefore we extended our study to assess whether DREADD chemogenetic activation of NTS_{POMC} neurons (CNO, 3mg/kg, i.p, Figure 4A-C), which may be considered as augmenting the ongoing activity in the circuit, also produced analgesia in the tail-flick and Hargreaves' assays. In the tail-flick assay, CNO administration increased withdrawal latency in $NTS_{POMC(Gq)}$ mice (CNO 3.1±0.25s vs NSS 1.9±0.22s, n=6, $p<0.05$, RM one-way ANOVA with Tukey's *post-hoc* test, Figure 4D). Naloxone treatment (1mg/kg, i.p) attenuated the analgesia produced by NTS_{POMC} chemo-activation (CNO + naloxone withdrawal latency 2.3±0.18s, n=6, $p<0.01$ vs CNO, Figure 4D) to a level comparable to baseline (p=0.17, Tukey's *post-hoc* test). In contrast, administration of CNO to control mice ($NTS_{POMC(Chrim)}$) had no effect on withdrawal latency in tail-flick assay (n=6, p=0.75, paired t-test, Figure 4E).

Similar analgesia was seen in the Hargreaves' test with chemo-activation prolonging latency to paw withdrawal in $NTS_{POMC(Gq)}$ mice (CNO 5.7±0.43s vs NSS 2.6±0.25s, n=6, $p<0.01$, RM one-way ANOVA with Tukey's *post-hoc* test, Figure 4F). Naloxone treatment reduced the analgesia produced by NTS_{POMC} chemo-activation (3.0±0.55s, $p<0.05$, Tukey's *post-hoc* test, Figure 4F) to a latency comparable to baseline (p=0.48, Tukey's *post-hoc* test). CNO administration to control mice ($NTS_{POMC(Chrim)}$) did not alter the withdrawal latency in Hargreaves' test (n=6, p=0.18, paired t-test, Figure 4G).

We next assessed whether chemogenetic activation of NTS_{POMC} neurons could ameliorate neuropathic or carrageenan-induced inflammatory pain behaviour (Figure 4H-I). Injection of carrageenan to the hind paw produced mechanical allodynia (von Frey) that developed over 3 hours (withdrawal force reduced to 0.13±0.05g from baseline 1.48±0.12g, $p<0.05$, RM one-way ANOVA with Tukey's *post-hoc* test, Figure 4J). CNO administration to $NTS_{POMC(Gq)}$ carrageenan mice attenuated the mechanical hypersensitivity (0.40±0.09g, $p<0.05$, Tukey's *post-hoc* test). This analgesic effect diminished over a period of 3 hours to

be statistically indistinguishable from the level of sensitisation pre-CNO injection (0.19±0.06g, Tukey's *post-hoc* test, Figure 4J). After TNT surgery, mice exhibited mechanical (von Frey) and cold (acetone) allodynia when tested 2-3 weeks after nerve transection ($p<0.01$, RM one-way ANOVA with Tukey's *post-hoc* test, Figure 4K-L). Administration of CNO to $NTS_{POMC(Gq)}$ TNT mice did not alter mechanical or cold allodynia ($p>0.05$, Tukey's *post-hoc* test).

3.8 Chemogenetic activation of NTS_{POMC} neurons does not produce aversion / preference

Given that we had observed that naloxone attenuated the analgesic effect of chemogenetic activation of NTS_{POMC} neurons (Section 3.7) suggesting the release of β-endorphin, therefore we tested for an affective valence. In CPP testing no significant difference was observed in the proportion of time spent in the CNO conditioned versus unconditioned chamber by the $NTS_{POMC(Gq)}$ animals (52.4±4.4 vs 47.6±4.4 %, n=6, p=0.45, Welch's t-test, Figure 5A-B). Moreover, the time spent in the conditioned chamber remained same before (during the 15 min habituation period) and after conditioning (47.0±2.4 vs 52.4±4.4%, p=0.31, Welch's t-test, Figure 5C).

3.9 Chemogenetic activation of NTS_{POMC} neurons is not anxiolytic.

To assess the effect of stimulation of NTS_{POMC} neurons on locomotion and anxiety-like behaviour we conducted an open field test. The $NTS_{POMC(Gq)}$ animals (n=5) spent similar time in the central arena compared to control animals ($NTS_{POMC(Chrim)}$, n=4) following CNO injection (p=0.82, Welch's t-test, Figure 5D). There was no difference between the groups in the distance travelled during the test (p=0.55, Welch's t-test, Figure 5E).

3.10 DREADD-mediated chemogenetic activation of NTS_{POMC} neurons does not cause respiratory depression

Synchronous optogenetic activation of NTS_{POMC} neurons produced respiratory pauses. We also found chemogenetic activation with PSAM produced respiratory depression (although as previously noted this was likely due to an off-target action of the $PSEM^{89s}$ agonist alone, Supplemental Figure 2). Therefore, spirometry was conducted in a plethysmography chamber to assess the effect of chemoactivation of NTS_{POMC} neurons upon respiration over a period of 1h after CNO (Figure 5F). No change in minute volume (% baseline) was observed after activation of NTS_{POMC} in comparison to NSS injection (n=5, p=0.94, two-way ANOVA).

Control mice did not show any change in minute volume with CNO dosing ($NTS_{POMC(Chrim)}$, n=2, p=0.97).

3.11 Chemogenetic inhibition of NTS_{POMC} neurons supresses stress-induced analgesia

Next, we explored the role of NTS_{POMC} neurons in stress-induced analgesia using an inhibitory chemogenetic strategy (Figure 6A-C). First, to determine whether inhibiting NTS_{POMC} neurons alters basal nociception we conducted tail-flick and Hargreaves' assays in $NTS_{POMC(Gi)}$ mice. Chemo-inhibition of NTS_{POMC} neurons had no effect on tail-flick withdrawal latency (CNO 2.30±0.14 vs NSS 2.37±0.14 s, n=6, p=0.51, paired t-test, Figure 6D&E) or Hargreaves' withdrawal latency (CNO 5.76±0.36 vs NSS 5.7±0.43 s, n=6, p=0.90, paired t-test, Figure 6F&G). Control animals given the same dose of CNO did not show any differences in these same tests ($NTS_{POMC(Chrim)}$, n=6, p>0.05, Figure 6E&G).

It has previously been shown that stress induced analgesia involves β-endorphin[47] but the identity of the neurons releasing the opioid peptide has not been identified. A 3-min swim induced analgesia with an increase in tail-flick latency (before swim 2.3±0.31 vs 4.43±0.33 s after swim, n=8, p=0.0002, Figure 6H). Administration of CNO to $NTS_{POMC(Gi)}$ mice before the swim significantly attenuated the increase in tail withdrawal latency (4.43±0.33 vs 3.2±0.28, p=0.025, RM one-way ANOVA with Tukey's *post-hoc* test, Figure 6H) returning it back towards the basal latency pre-swim (no longer statistically different from baseline, p=0.12, Tukey's *post-hoc* test, Figure 6H). Stress induced analgesia was also observed in control $NTS_{POMC(Chrim)}$ mice (n=4, p=0.01, RM one-way ANOVA with Tukey's *post-hoc* test) but CNO injection had no effect on this analgesic action (p=0.9, Tukey's *post-hoc* test, Figure 6I).

3.12 Chemogenetic inhibition of ARC_{POMC} neurons does not attenuate stress-induced analgesia

The other major site of POMC synthesis in the CNS is in the ARC (Supplemental Figure 5A-C). We undertook proof of principle experiments to test whether chemogenetic inhibition of POMC neurons located in the ARC had any impact on stress analgesia. A 3-min swim again induced a significant (p=0.02) increase in tail flick latency in $ARC_{POMC(Gi)}$ mice, but prior CNO administration did not alter this stress induced analgesia (n=3, p>0.05, RM one-way ANOVA with Tukey's *post-hoc* test, Supplemental Figure 5D-E).

In all the above experiments *post-hoc* histology confirmed transduction of neurons with a pattern and distribution consistent with them being NTS_{POMC} or ARC $_{POMC}$ neurons (Supplemental Figure 1B and 5C, Figure 2D, 4E & 6C)[13].

4 Discussion

Opto- or chemo-genetic activation of NTS_{POMC} neurons produces a sustained analgesia that is in part mediated by endogenous opioid release. Opto-stimulation of this neuronal population also produces a transient bradycardia and bradypnoea. The chemogenetic activation of NTS_{POMC} neuron is well-tolerated by the mice as they exhibit no respiratory depression, aversion/preference, anxiolysis or locomotor consequences. We establish that the NTS_{POMC} neurons, but not the hypothalamic ARC_{POMC} neurons, play a role in stress-induced analgesia which can be blocked by chemogenetic inhibition. This corroborates and extends our previous observations made using the PSAM chemogenetic method[13] and identifies the NTS_{POMC} neurons as a key component of endogenous analgesic circuity.

Activation of NTS_{POMC} neurons resulted in opioid mediated analgesia consistent with the principle that these NTS neurons release β-endorphin. Brief opto-activation of NTS_{POMC} neurons in freely behaving mice showed an analgesia action in Hargreaves' and tail-flick assays that lasted for 30 mins and was 70-75% blocked by naloxone. A previous study reported approximately 40% maximum possible analgesia (MPE) in tail-flick assay after morphine injection (10 mg/kg, s.c) in mice[10]. Interestingly, in our study, if we calculate the MPE due to opto-activation of the NTS_{POMC} neurons in the tail-flick assay, it stands around 90%. Although this direct comparison is hampered by different study designs, nonetheless this shows a powerful endogenous analgesic effect. The presence of a residual analgesic effect (~25%) following NTS_{POMC} neuron activation after naloxone may indicate that other mechanisms besides endogenous opioids are involved or alternatively that the dose of naloxone was not sufficient to completely block the actions of focally-released β-endorphin.

Using an excitatory DREADD chemogenetic approach we again identified an opioid-mediated analgesic effect in acute pain models. These findings are in line with prior observations, using a different chemogenetic strategy, that showed NTS_{POMC} activation produced analgesia[13]. We also show that this analgesic effect is seen in an acute carrageenan model of inflammatory mechanical sensitisation but not in a neuropathic pain model. This mirrors the known beneficial actions of opioids in inflammatory pain but not neuropathic pain

where they are markedly less beneficial[16;40;58]. It remains to be determined whether this apparent lack of a role in a chronic neuropathic pain model also applies to other models of chronic pain. Opioid mediated analgesia has also been reported following electrical or direct chemical stimulation of NTS[2;36] and our study extends these findings to indicate that focal activation of the small population of ~200 NTS_{POMC} neurons can produce powerful opioid-mediated analgesia.

β-endorphin has been shown to play a role in stress-induced analgesia[12;38;47] so we tested the hypothesis that NTS_{POMC} neurons may be the source of the β-endorphin that mediates stress evoked analgesia. Chemogenetic inhibition of NTS_{POMC} neurons did not produce any change in basal nociception in both the Hargreaves' and tail-flick assays – suggesting that there is no analgesic tone in the system under baseline conditions. However inhibiting NTS_{POMC} neurons (but not those in the arcuate) attenuated swim stress-induced analgesia. This result confirms that stress induced analgesia is mediated by β-endorphin and identified the NTS_{POMC} as a core node in the network. The NTS is a key integrating station for afferents from the viscera and from muscles[11] and is therefore well positioned to co-ordinate and mediate exercise-induced changes in sensory processing. The NTS_{POMC} neurons project into the region of the rostro-medial medulla as well as up to the ventral PAG[13] which would be a potential link for the NTS_{POMC} neurons into the descending pain modulation system[39]. It is also possible that these neurons could play a role in vagal stimulation-evoked analgesia[1] that is increasingly used as a therapeutic treatment for pain conditions like migraine[49;52], but this remains to be tested.

Opto-activating NTS_{POMC} neurons produced transient bradycardia *in vivo* with similar characteristics to that found in the working heart-brainstem preparation[13]. Naloxone reduced the effect of opto-stimulation which suggests that the bradycardia was in part opioid-mediated and likely due to release of β-endorphin. The NTS_{POMC} neurons project to nucleus ambiguus (NA) in close proximity to the cholinergic cardiac vagal preganglionic neurons (CVNs) neurons[13;55]. The excitation of CVNs with vagal activation can generate a bradycardia[8;25;41]. Opioids characteristically inhibit postsynaptic neurons via their cognate G-protein coupled receptors[15;27], and so this is not consistent with a direct synapse from NTS_{POMC} neurons directly onto CVNs. However a fast inhibition of CVNs by adjacent interneurons has been reported[17]. Additionally, such GABAergic/glycinergic interneurons have been shown to be inhibited by exogenous opioids *in vitro*[19;54]. This suggests a potential mechanism whereby β-endorphins released from the POMC neurons inhibit the

presynaptic inhibitory interneurons to disinhibit the CVNs and cause bradycardia. There is also evidence for glutamate expressing POMC neurons in the arcuate nucleus of the hypothalamus[21;26]. Therefore, it is also plausible that the bradycardia seen following activation of NTS_{POMC} neurons could be due to a dual mechanism involving direct glutamatergic excitation and β-endorphin mediated disinhibition. Distinguishing between these circuit hypotheses will likely require cellular resolution recording studies from vagal preganglionic neurons.

Since we observed transient respiratory pauses following synchronous opto-stimulation of NTS_{POMC} neurons (similar to that seen in the working heart brainstem preparation,[13]) we aimed to assess if chemogenetic activation also produced respiratory depression. Spirometry showed no sign of changes in minute volume following activation of the NTS_{POMC} neurons with a CNO dose that produced analgesia. The axons of the NTS_{POMC} neurons are known to be distributed across the ventral respiratory column and ascend to the vicinity of the Kölliker-Fuse nucleus[13;55], both of which are known to be involved in opioid mediated regulation of respiratory pattern[35;43]. Therefore, the necessary connectivity for these respiratory actions is present and it is likely that the difference in respiratory effects between opto- and chemogenetic activation relates to the pattern of activity that is triggered. Optoactivation imposes an abrupt synchronous discharge of the NTS_{POMC} neurons at an exogenous, arbitrary frequency. In contrast the chemogenetic activation modulates the excitability of the NTS_{POMC} neurons augmenting their natural firing pattern which may be less likely to produce the respiratory suppression. Chemogenetic activation does produce an opioid-like analgesic effect likely via the release of β-endorphin so the lack of respiratory depression cannot be explained on the basis of a differential release of opioid by each stimulation mechanism. This may indicate that there is a therapeutic window for chemogenetic activation of NTS_{POMC} neurons that reduces the risk of respiratory depression.

Our study employed opto- and chemo-genetic approaches to alter the intrinsic activity of the POMC neurons. Such approaches require controls both within animal and across groups to take account of potential off target effects of chemogenetic ligand or non-specific effects of blue light. We designed an efficient control group strategy using a similar AAV vector to express the chemogenetic actuator and a fluorophore for the optogenetic experiments and vice-versa for chemogenetic experiments. This provided control for the effects of vector infection, expression of membrane bound actuator protein and fluorophore and enabled blinding of experimenters. This approach offers advantages over the more commonly employed strategy

of just expressing a fluorophore using a Cre-dependent AAV. Our approach, however, introduces a possible confound that the actuator expression in the control group may change the excitability/function of the POMC neurons under basal conditions[18;48]. We found no evidence of changes in between group comparisons across multiple measures, however, to rule out this possibility definitively would require detailed cellular electrophysiology which was beyond the scope of our study. We also note that throughout the study there was consistency between approaches using the different opto- and chemo-genetic actuators to change the activity in the POMC neurons which would not have been expected if expression of the actuators was having a detrimental effect on function.

Systemic opioids are associated with a spectrum of other serious side effects besides respiratory depression including addiction linked to reward, sedation and anxiolysis as well as nausea and aversion/dysphoria[15]. Therefore, we sought to assess whether there was any evidence for similar actions with activation of NTS_{POMC} neurons. We found no evidence of either preference nor aversion from the opto- or chemo- activation in the conditioned place preference assays which suggest activation of these neurons does not produce a strong affective valence. Similarly, in the open field test there were no changes in either the time spent in the central zone of the arena (a measure of anxiety) or in the total distance travelled following chemo-activation. These null findings in assays of preference, anxiety-like and locomotor behaviour from levels of activation that produced analgesic effects again are consistent with the idea that focal opioid release produced by direct activation of an opioid releasing circuit can minimise unwanted effects. This is analogous to a more selective version of deep brain stimulation which has been shown to focally release opioids in the periaqueductal grey[50], without some of the typical side effects seen with systemic opioids.

5 Conclusion

Overall, our study shows that opto-stimulation of NTS_{POMC} neurons produces transient cardio-respiratory depression in anaesthetised mice. We demonstrate that both opto- and chemogenetic activation of NTS_{POMC} neurons produces a sustained strong analgesia without evidence of adverse effects. We also provide evidence that this small population of medullary POMC neurons plays a central role in stress-induced analgesia.

6 Conflict of interest statement

The authors have no conflicts of interest to declare.

7 Acknowledgement

This work was funded by Medical Research Council (ref: MR/P025749/1). For the purpose of open access, the author has applied a 'Creative Commons Attribution (CC BY) public copyright licence to any Author Accepted Manuscript (AAM) version arising from this submission. The source data for the paper is openly available from data.bris at DOI 10.5523/bris.3mricoucwoop82ka13go8scs26. AEP has grant funding from Eli Lilly and provided consultancy to Eli Lilly and Lateral Pharma unrelated to this study.

8 References

[1] Aicher SA, Lewis SJ, Randich A. Antinociception produced by electrical stimulation of vagal afferents: independence of cervical and subdiaphragmatic branches. Brain Res 1991;542(1):63-70.

[2] Aicher SA, Randich A. Antinociception and cardiovascular responses produced by electrical stimulation in the nucleus tractus solitarius, nucleus reticularis ventralis, and the caudal medulla. Pain 1990;42(1):103-119.

[3] Anderson EJ, Cakir I, Carrington SJ, Cone RD, Ghamari-Langroudi M, Gillyard T, Gimenez LE, Litt MJ. 60 YEARS OF POMC: Regulation of feeding and energy homeostasis by alpha-MSH. J Mol Endocrinol 2016;56(4):T157-174.

[4] Baizman ER, Cox BM. Endorphin in rat pituitary glands: its distribution within the gland, and age related changes in gland content in male and female rats. Life Sci 1978;22(6):519-526.

[5] Balthasar N, Coppari R, McMinn J, Liu SM, Lee CE, Tang V, Kenny CD, McGovern RA, Chua SC, Jr., Elmquist JK, Lowell BB. Leptin receptor signaling in POMC neurons is required for normal body weight homeostasis. Neuron 2004;42(6):983-991.

[6] Balthasar N, Dalgaard LT, Lee CE, Yu J, Funahashi H, Williams T, Ferreira M, Tang V, McGovern RA, Kenny CD, Christiansen LM, Edelstein E, Choi B, Boss O, Aschkenasi C, Zhang CY, Mountjoy K, Kishi T, Elmquist JK, Lowell BB. Divergence of melanocortin pathways in the control of food intake and energy expenditure. Cell 2005;123(3):493-505.

[7] Bicknell AB. The tissue-specific processing of pro-opiomelanocortin. J Neuroendocrinol 2008;20(6):692-699.

[8] Bieger D, Hopkins DA. Viscerotopic representation of the upper alimentary tract in the medulla oblongata in the rat: the nucleus ambiguus. J Comp Neurol 1987;262(4):546-562.

[9] Boecker H, Sprenger T, Spilker ME, Henriksen G, Koppenhoefer M, Wagner KJ, Valet M, Berthele A, Tolle TR. The runner's high: opioidergic mechanisms in the human brain. Cerebral cortex 2008;18(11):2523-2531.

[10] Bohn LM, Lefkowitz RJ, Caron MG. Differential mechanisms of morphine antinociceptive tolerance revealed in (beta)arrestin-2 knock-out mice. J Neurosci 2002;22(23):10494-10500.

[11] Boscan P, Pickering AE, Paton JF. The nucleus of the solitary tract: an integrating station for nociceptive and cardiorespiratory afferents. Exp Physiol 2002;87(2):259-266.

[12] Butler RK, Finn DP. Stress-induced analgesia. Prog Neurobiol 2009;88(3):184-202.

[13] Cerritelli S, Hirschberg S, Hill R, Balthasar N, Pickering AE. Activation of Brainstem Pro-opiomelanocortin Neurons Produces Opioidergic Analgesia, Bradycardia and Bradypnoea. PLoS One 2016;11(4):e0153187.

[14] Contet C, Gavériaux-Ruff C, Matifas A, Caradec C, Champy MF, Kieffer BL. Dissociation of analgesic and hormonal responses to forced swim stress using opioid receptor knockout mice. Neuropsychopharmacology 2006;31(8):1733-1744.

[15] Corbett AD, Henderson G, McKnight AT, Paterson SJ. 75 years of opioid research: the exciting but vain quest for the Holy Grail. Br J Pharmacol 2006;147 Suppl 1:S153-162.

[16] Finnerup NB, Attal N, Haroutounian S, McNicol E, Baron R, Dworkin RH, Gilron I, Haanpaa M, Hansson P, Jensen TS, Kamerman PR, Lund K, Moore A, Raja SN, Rice AS, Rowbotham M, Sena E, Siddall P, Smith BH, Wallace M. Pharmacotherapy for neuropathic pain in adults: a systematic review and meta-analysis. Lancet Neurol 2015;14(2):162-173.

[17] Frank JG, Jameson HS, Gorini C, Mendelowitz D. Mapping and identification of GABAergic neurons in transgenic mice projecting to cardiac vagal neurons in the nucleus ambiguus using photo-uncaging. J Neurophysiol 2009;101(4):1755-1760.
[18] Goutaudier R, Coizet V, Carcenac C, Carnicella S. DREADDs: The Power of the Lock, the Weakness of the Key. Favoring the Pursuit of Specific Conditions Rather than Specific Ligands. eNeuro 2019;6(5).
[19] Griffioen KJ, Venkatesan P, Huang ZG, Wang X, Bouairi E, Evans C, Gold A, Mendelowitz D. Fentanyl inhibits GABAergic neurotransmission to cardiac vagal neurons in the nucleus ambiguus. Brain Res 2004;1007(1-2):109-115.
[20] Hargreaves K, Dubner R, Brown F, Flores C, Joris J. A new and sensitive method for measuring thermal nociception in cutaneous hyperalgesia. Pain 1988;32(1):77-88.
[21] Hentges ST, Otero-Corchon V, Pennock RL, King CM, Low MJ. Proopiomelanocortin expression in both GABA and glutamate neurons. J Neurosci 2009;29(43):13684-13690.
[22] Hughes S, Hickey L, Donaldson LF, Lumb BM, Pickering AE. Intrathecal reboxetine suppresses evoked and ongoing neuropathic pain behaviours by restoring spinal noradrenergic inhibitory tone. Pain 2015;156(2):328-334.
[23] Hughes SW, Hickey L, Hulse RP, Lumb BM, Pickering AE. Endogenous analgesic action of the pontospinal noradrenergic system spatially restricts and temporally delays the progression of neuropathic pain following tibial nerve injury. Pain 2013;154(9):1680-1690.
[24] Huo L, Grill HJ, Bjorbaek C. Divergent regulation of proopiomelanocortin neurons by leptin in the nucleus of the solitary tract and in the arcuate hypothalamic nucleus. Diabetes 2006;55(3):567-573.
[25] Izzo PN, Deuchars J, Spyer KM. Localization of cardiac vagal preganglionic motoneurones in the rat: immunocytochemical evidence of synaptic inputs containing 5-hydroxytryptamine. J Comp Neurol 1993;327(4):572-583.
[26] Jarvie BC, Hentges ST. Expression of GABAergic and glutamatergic phenotypic markers in hypothalamic proopiomelanocortin neurons. J Comp Neurol 2012;520(17):3863-3876.
[27] Jordan BA, Cvejic S, Devi LA. Opioids and Their Complicated Receptor Complexes. Neuropsychopharmacology : official publication of the American College of Neuropsychopharmacology 2000;23(1):S5-S18.
[28] Klapoetke NC, Murata Y, Kim SS, Pulver SR, Birdsey-Benson A, Cho YK, Morimoto TK, Chuong AS, Carpenter EJ, Tian Z, Wang J, Xie Y, Yan Z, Zhang Y, Chow BY, Surek B, Melkonian M, Jayaraman V, Constantine-Paton M, Wong GK, Boyden ES. Independent optical excitation of distinct neural populations. Nat Methods 2014;11(3):338-346.
[29] Krashes MJ, Koda S, Ye C, Rogan SC, Adams AC, Cusher DS, Maratos-Flier E, Roth BL, Lowell BB. Rapid, reversible activation of AgRP neurons drives feeding behavior in mice. J Clin Invest 2011;121(4):1424-1428.
[30] Lee BH, Won R, Baik EJ, Lee SH, Moon CH. An animal model of neuropathic pain employing injury to the sciatic nerve branches. Neuroreport 2000;11(4):657-661.
[31] Lewis JW, Baldrighi G, Akil H. A possible interface between autonomic function and pain control: opioid analgesia and the nucleus tractus solitarius. Brain Res 1987;424(1):65-70.
[32] Magnus CJ, Lee PH, Atasoy D, Su HH, Looger LL, Sternson SM. Chemical and genetic engineering of selective ion channel-ligand interactions. Science 2011;333(6047):1292-1296.

[33] McCarson KE, Fehrenbacher JC. Models of Inflammation: Carrageenan- or Complete Freund's Adjuvant (CFA)-Induced Edema and Hypersensitivity in the Rat. Curr Protoc 2021;1(7):e202.
[34] Millan MJ. Multiple opioid systems and pain. Pain 1986;27(3):303-347.
[35] Montandon G, Qin W, Liu H, Ren J, Greer JJ, Horner RL. PreBotzinger complex neurokinin-1 receptor-expressing neurons mediate opioid-induced respiratory depression. J Neurosci 2011;31(4):1292-1301.
[36] Morgan MM, Sohn JH, Lohof AM, Ben-Eliyahu S, Liebeskind JC. Characterization of stimulation-produced analgesia from the nucleus tractus solitarius in the rat. Brain Res 1989;486(1):175-180.
[37] Morgan WP. Affective beneficence of vigorous physical activity. Med Sci Sports Exerc 1985;17(1):94-100.
[38] Nakagawasai O, Tadano T, Tan No K, Niijima F, Sakurada S, Endo Y, Kisara K. Changes in beta-endorphin and stress-induced analgesia in mice after exposure to forced walking stress. Methods Find Exp Clin Pharmacol 1999;21(7):471-476.
[39] Ossipov MH, Dussor GO, Porreca F. Central modulation of pain. J Clin Invest 2010;120(11):3779-3787.
[40] Ossipov MH, Kovelowski CJ, Porreca F. The increase in morphine antinociceptive potency produced by carrageenan-induced hindpaw inflammation is blocked by naltrindole, a selective delta-opioid antagonist. Neurosci Lett 1995;184(3):173-176.
[41] Palkovits M, Mezey E, Eskay RL. Pro-opiomelanocortin-derived peptides (ACTH/beta-endorphin/alpha-MSH) in brainstem baroreceptor areas of the rat. Brain Res 1987;436(2):323-338.
[42] Pisanello F, Mandelbaum G, Pisanello M, Oldenburg IA, Sileo L, Markowitz JE, Peterson RE, Della Patria A, Haynes TM, Emara MS, Spagnolo B, Datta SR, De Vittorio M, Sabatini BL. Dynamic illumination of spatially restricted or large brain volumes via a single tapered optical fiber. Nat Neurosci 2017;20(8):1180-1188.
[43] Prkic I, Mustapic S, Radocaj T, Stucke AG, Stuth EA, Hopp FA, Dean C, Zuperku EJ. Pontine μ-opioid receptors mediate bradypnea caused by intravenous remifentanil infusions at clinically relevant concentrations in dogs. J Neurophysiol 2012;108(9):2430-2441.
[44] Radosevich PM, Nash JA, Lacy DB, O'Donovan C, Williams PE, Abumrad NN. Effects of low- and high-intensity exercise on plasma and cerebrospinal fluid levels of ir-beta-endorphin, ACTH, cortisol, norepinephrine and glucose in the conscious dog. Brain Res 1989;498(1):89-98.
[45] Richardson D, Gunton H, West H, Rachel G, Ian M, Janet N, Laura C, Burgess G. Tibial Nerve Transection (TNT) Model of Neuropathic Pain in the Rat, 2015.
[46] Roth BL. DREADDs for Neuroscientists. Neuron 2016;89(4):683-694.
[47] Rubinstein M, Mogil JS, Japon M, Chan EC, Allen RG, Low MJ. Absence of opioid stress-induced analgesia in mice lacking beta-endorphin by site-directed mutagenesis. Proc Natl Acad Sci U S A 1996;93(9):3995-4000.
[48] Saloman JL, Scheff NN, Snyder LM, Ross SE, Davis BM, Gold MS. Gi-DREADD Expression in Peripheral Nerves Produces Ligand-Dependent Analgesia, as well as Ligand-Independent Functional Changes in Sensory Neurons. J Neurosci 2016;36(42):10769-10781.
[49] Silberstein SD, Calhoun AH, Lipton RB, Grosberg BM, Cady RK, Dorlas S, Simmons KA, Mullin C, Liebler EJ, Goadsby PJ, Saper JR. Chronic migraine headache prevention with noninvasive vagus nerve stimulation: The EVENT study. Neurology 2016;87(5):529-538.

[50] Sims-Williams H, Matthews JC, Talbot PS, Love-Jones S, Brooks JC, Patel NK, Pickering AE. Deep brain stimulation of the periaqueductal gray releases endogenous opioids in humans. Neuroimage 2017;146:833-842.
[51] Stein L, Belluzzi JD. Brain endorphins: possible role in reward and memory formation. Fed Proc 1979;38(11):2468-2472.
[52] Tassorelli C, Grazzi L, de Tommaso M, Pierangeli G, Martelletti P, Rainero I, Dorlas S, Geppetti P, Ambrosini A, Sarchielli P, Liebler E, Barbanti P. Noninvasive vagus nerve stimulation as acute therapy for migraine: The randomized PRESTO study. Neurology 2018;91(4):e364-e373.
[53] van den Pol AN, Acuna C, Davis JN, Huang H, Zhang X. Defining the caudal hypothalamic arcuate nucleus with a focus on anorexic excitatory neurons. J Physiol 2019;597(6):1605-1625.
[54] Venkatesan P, Baxi S, Evans C, Neff R, Wang X, Mendelowitz D. Glycinergic inputs to cardiac vagal neurons in the nucleus ambiguus are inhibited by nociceptin and mu-selective opioids. J Neurophysiol 2003;90(3):1581-1588.
[55] Wang D, He X, Zhao Z, Feng Q, Lin R, Sun Y, Ding T, Xu F, Luo M, Zhan C. Whole-brain mapping of the direct inputs and axonal projections of POMC and AgRP neurons. 2015;9(40).
[56] Yizhar O, Fenno LE, Davidson TJ, Mogri M, Deisseroth K. Optogenetics in neural systems. Neuron 2011;71(1):9-34.
[57] Zhan C, Zhou J, Feng Q, Zhang JE, Lin S, Bao J, Wu P, Luo M. Acute and long-term suppression of feeding behavior by POMC neurons in the brainstem and hypothalamus, respectively. J Neurosci 2013;33(8):3624-3632.
[58] Zhang X-Y, Dou Y-N, Yuan L, Li Q, Zhu Y-J, Wang M, Sun Y-G. Different neuronal populations mediate inflammatory pain analgesia by exogenous and endogenous opioids. eLife 2020;9:e55289.

Figure Legends

Figure 1. Optogenetic activation of NTS POMC neurons expressing ChrimsonR A. Example ChrimsonR-tdTomato positive POMC neuron in an acute medullary slice targeted for whole-cell patch clamp recordings. Dashed lines indicate pipette location. **B_1** ChrimsonR-mediated inward photocurrent in response to a 100ms light pulse (620nm, -60mV holding potential). **B_2** Plot of ChrimsonR current amplitudes from 7 neurons (as B_1). **C** Optogenetic activation of ChrimsonR drives action potentials in POMC neurons **C_1** 5ms at 5Hz, **C_2** 20ms at 5Hz and **C_3** 5ms at 20Hz.

Figure 2. Cardiorespiratory effect of opto-stimulation of NTS_{POMC} neurons in chronically implanted mice A. Timeline for optogenetic experiments in implanted mice (pain tests and CPP data shown in Figure 3). **B.** Injection of AAV-ChrimsonR-tdTomato into the NTS of POMC-Cre mice **C.** Schematic diagram shows opto-stimulation of NTS_{POMC} neurons via wireless LED attached to optic fibre (20ms × 5-20 Hz, 5s). Representative histological section of brain stem shows **D1.** NTS_{POMC} neurons expressing tdTomato **D2.** optic fibre location (OF) in the NTS in ChrimsonR-tdTomato injected mice **E.** Opto-stimulation in $NTS_{POMC(Chrim)}$ mice (n=6) produced bradycardia at 5Hz (15.2% vs 3.2%), 10Hz (38.7% vs 1.9%) and 20Hz (51.7% vs 1.9%) compared to baseline. Heart rate returned to baseline values during recovery period (within 10 seconds) **F.** Opto-stimulation produced no bradycardia in control implanted $NTS_{POMC(Dq)}$ mice (n=4). **G.** Opto-stimulation at all frequencies (2-20 Hz) in $NTS_{POMC(Chrim)}$ mice (n=6) produced bradypnoea (35.9% vs 7.4%, 168.9% vs 7%, 367.1% vs 5.5%, 440.7% vs 6.2% respectively) compared to baseline values. The respiratory rate returned to baseline values within 10s of the end of illumination. **H.** Opto-stimulation did not affect respiratory rate in control $NTS_{POMC(Dq)}$ mice (n=4) **I, J.** The ΔBradycardia and ΔBradypnoea in $NTS_{POMC(Chrim)}$ mice (n=6) was dependent on opto-stimulation frequency. Data presented as median, min to max and analysed by Friedman test with Dunn's *post-hoc* test. *P<0.05, **p<0.01, ***p<0.001.

Figure 3. Effect of opto-stimulation of NTS_{POMC} neurons on analgesia and preference/avoidance. A. Timeline for optogenetic experiments in implanted in implanted

$NTS_{POMC(Chrim)}$ mice. Opto-stimulation of NTS_{POMC} neurons (20ms pulse at 5Hz for 1 min) produced increased withdrawal latency in both the tail flick test **(B.)** and Hargreaves' test **(D.)** which was reduced by opioid antagonist naloxone (n=6, RM one-way ANOVA with Tukey's *post-hoc* test). Identical opto-stimulation in implanted control vector injected mice had no effect on latencies in either the tail-flick test **(C.)** or the Hargreaves' test **(E.)** (n=6, paired t-test). **F.** Time course of analgesia assessed in Hargreaves' test. A sustained analgesia was observed until 30 min post-activation of these neurons (n=6, RM one-way ANOVA with Tukey's *post-hoc* test). **G.** Conditioned place preference testing showed that opto-stimulation in $NTS_{POMC(Chrim)}$ mice had no significant effect on the time spent in opto-stimulation conditioned vs unconditioned chamber (assessed after conditioning, n=6, Welch's t-test) or **H.** on the time spent before (15 min habituation period) vs after conditioning (15 min test period) in conditioned chamber (paired t-test). Data are presented as mean ± SE. *p<0.05, **p<0.01, ***p<0.001, ****p<0.0001.

Figure 4. Chemogenetic activation of NTS_{POMC} neurons is analgesic in acute thermal and inflammatory pain models but not in a neuropathic model. A. Timeline for acute chemogenetic experiments **B.** Schematic diagram shows injection of AAV-hM3Dq-mcherry into the NTS of POMC-Cre mice. **C.** Representative histological section of brain stem shows NTS_{POMC} neurons expressing mCherry in $NTS_{POMC(Gq)}$ mice. Chemogenetic activation in $NTS_{POMC(Gq)}$ mice with CNO (3mg/kg, i.p) produced increased **D**. tail flick and **F.** paw withdrawal latencies, respectively, which were blocked by the opioid antagonist naloxone (1mg/kg, i.p) (n=6, RM one-way ANOVA with Tukey's *post-hoc* test). In contrast CNO showed no effect in control $NTS_{POMC(Chrim)}$ mice in the **E.** Tail-flick test (n=6) or **G.** Hargreaves' test (n=6) (paired t-test). H. Timeline for carrageenan-induced inflammatory pain experiment **I.** Timeline for TNT induced neuropathic pain experiment. **J.** Hind paw injection of carrageenan produced mechanical allodynia that was evident with control NSS injection (von Frey, 3.5 hours post carrageenan). Chemoactivation of the NTS_{POMC} neurons (CNO 3mg/kg, i.p, 5 hours post carrageenan) significantly increased the paw withdrawal threshold (n=5, p<0.05, one-way ANOVA with Tukey's *post-hoc* test). The sensitisation returned on retesting 2.5 hours after CNO. **K.** After TNT surgery the $NTS_{POMC(Gq)}$ mice exhibit mechanical allodynia (von Frey assessed after 3 weeks) but subsequent CNO injection (3mg/kg, i.p) has no effect on paw withdrawal threshold (n=6, p>0.05, one-way ANOVA with Tukey's *post-hoc* test). **L.** Acetone testing showed cold allodynia in $NTS_{POMC(Gq)}$ TNT mice with an increase in

the number of nocifensive responses in one minute (tested 2 weeks after TNT). Again, CNO injection (3mg/kg, i.p) had no effect on acetone evoked nocifensive responses (n=5, $p>0.05$, one-way ANOVA with Tukey's *post-hoc* test). For K and L, CNO or NSS were administered on consecutive days (counterbalanced design and experimenter blinded to drug). Each value is an average of three measures. In each trial testing was done 15 mins after injection of CNO/NSS. Data are presented as mean ± SE. *$p<0.05$, **$p<0.01$, ***$p<0.001$.

Figure 5. Chemoactivation of NTS_{POMC} neurons has no aversive, anxiogenic, locomotor or respiratory depressant actions. A. Timeline for chemogenetic experiments. The affective valence of chemogenetic activation of NTS_{POMC} neurons was assessed in a conditioned place preference test which showed no difference in either **B.** Proportion of time spent in CNO conditioned vs unconditioned chamber (n=6, Welch's t-test) or **C.** Percentage of time spent in CNO chamber before vs after the conditioning (paired t-test). To identify any change in anxiety-like behaviour the $NTS_{POMC(Gq)}$ mice were tested in an open field arena. **D.** No difference was observed in the time spent in the central zone of the arena by $NTS_{POMC(Gq)}$ mice (n=5) compared to control $NTS_{POMC(Chrim)}$ mice (n=4) following CNO (3mg/kg, i.p, $p>0.05$, Welch's t-test). **E.** No change was observed in the distance travelled by the $NTS_{POMC(Gq)}$ compared to control mice following CNO injection (3mg/kg, i.p, $p>0.05$, Welch's t-test). To test for respiratory depression associated with chemogenetic activation of NTS_{POMC} neurons the animals had whole body plethysmography **F.** No difference was observed in minute volume (% baseline) of the $NTS_{POMC(Gq)}$ animals following CNO (3mg/kg, i.p) compared to NSS (n=5, $p>0.05$, two-way ANOVA). Data are presented as mean ± SE. *$p<0.05$, **$p<0.01$.

Figure 6. Effect of chemogenetic inhibition of NTS_{POMC} neurons on nociception and stress-induced analgesia. A. Timeline for NTS_{POMC} inhibitory chemogenetic experiments. **B.** Schematic diagram shows injection of AAV2 hM4Di-mcherry into the NTS of POMC-Cre mice. **C.** Representative histological section of brain stem shows NTS_{POMC} neurons expressing mCherry. CNO injection (3mg/kg, i.p) did not produce any effect in $NTS_{POMC(Gi)}$ mice (n=6) under basal conditions in the **D**. Tail-flick test or **F.** Hargreaves' test (paired t-test). CNO injection to control $NTS_{POMC(Chrim)}$ mice (n=6) showed no effect on **E.** Tail-flick test (same data as Figure 4G) and **G.** Hargreaves' test (paired t-test). **H.** A significant increase in tail

withdrawal threshold was observed in $NTS_{POMC(Gi)}$ mice following a brief swim which was attenuated by CNO injection (n=8, RM one-way ANOVA with Tukey's *post-hoc* test). **I.** Stress induced analgesia was also observed in $NTS_{POMC(Chrim)}$ mice and CNO failed to alter this effect (n=4, RM one-way ANOVA with Tukey's *post-hoc* test).

Data are presented as mean ± SE.*p<0.05, **p<0.01 ***p<0.001.

Figure 1

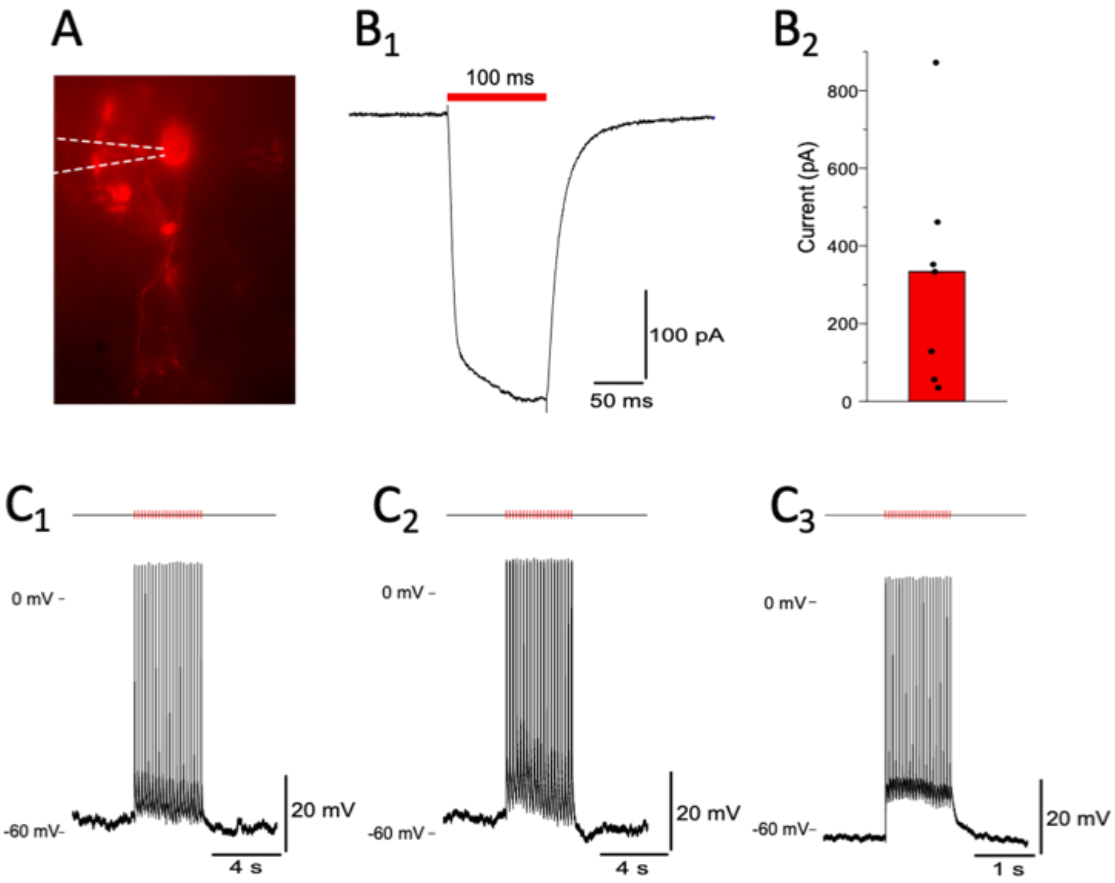
A
B1
100 ms
100 pA
50 ms
B2
Current (pA)
800
600
400
200
0
C1
0 mV
-60 mV
20 mV
4 s
C2
0 mV
-60 mV
20 mV
4 s
C3
0 mV
-60 mV
20 mV
1 s

Figure 2

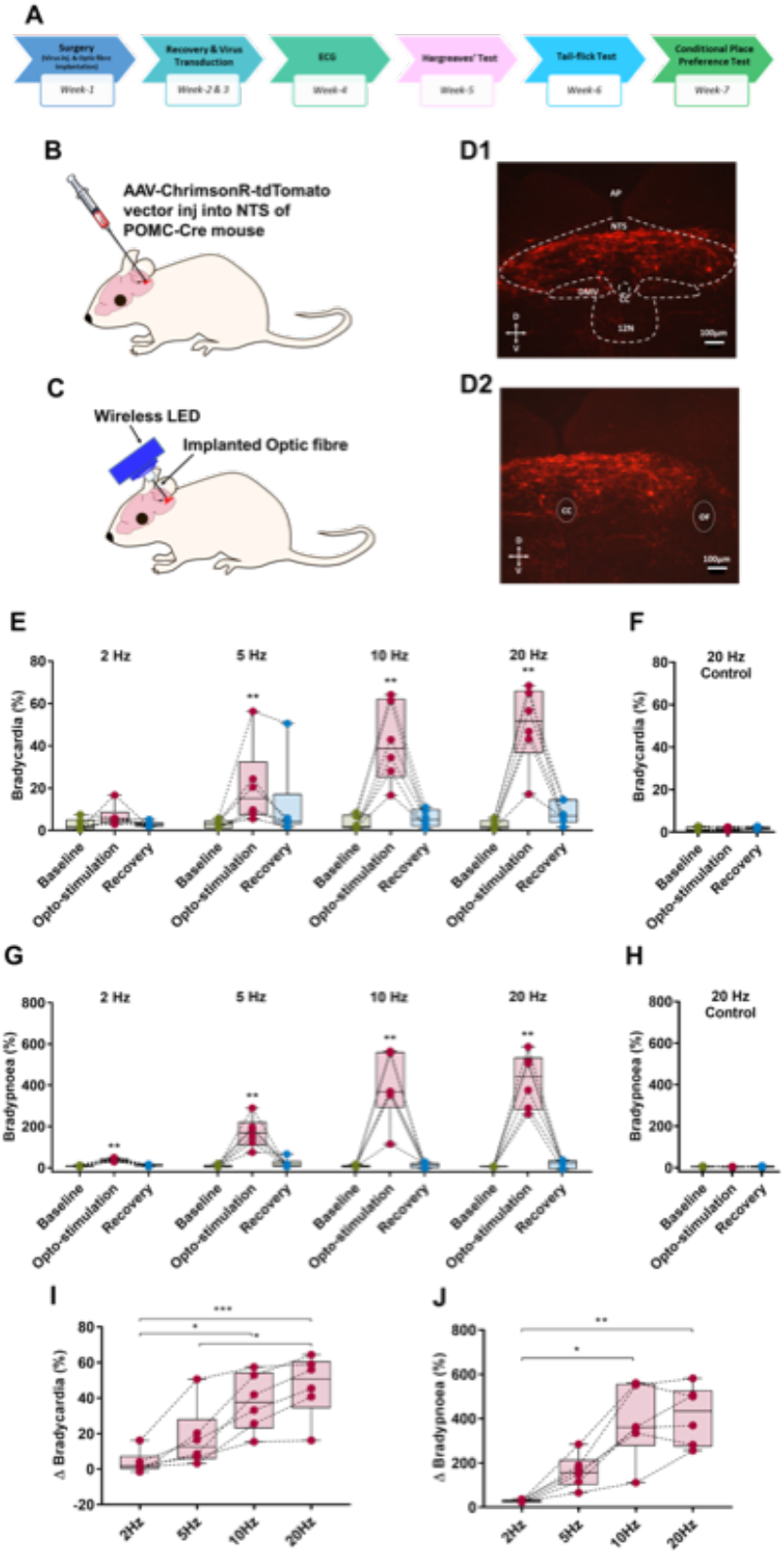
A
Surgery
Recovery & Virus Transduction
ECG
Hargreaves' Test
Tail-flick Test
Conditional Place Preference Test
Week-1
Week-2 & 3
Week-4
Week-5
Week-6
Week-7
B
AAV-ChrimsonR-tdTomato vector inj into NTS of POMC-Cre mouse
C
Wireless LED
Implanted Optic fibre
D1
D2
AP
NTS
12N
100μm
E
2 Hz
5 Hz
10 Hz
20 Hz
Bradycardia (%)
Baseline
Opto-stimulation
Recovery
F
20 Hz Control
G
Bradypnoea (%)
H
I
Δ Bradycardia (%)
2Hz
5Hz
10Hz
20Hz
J
Δ Bradypnoea (%)

Figure 3

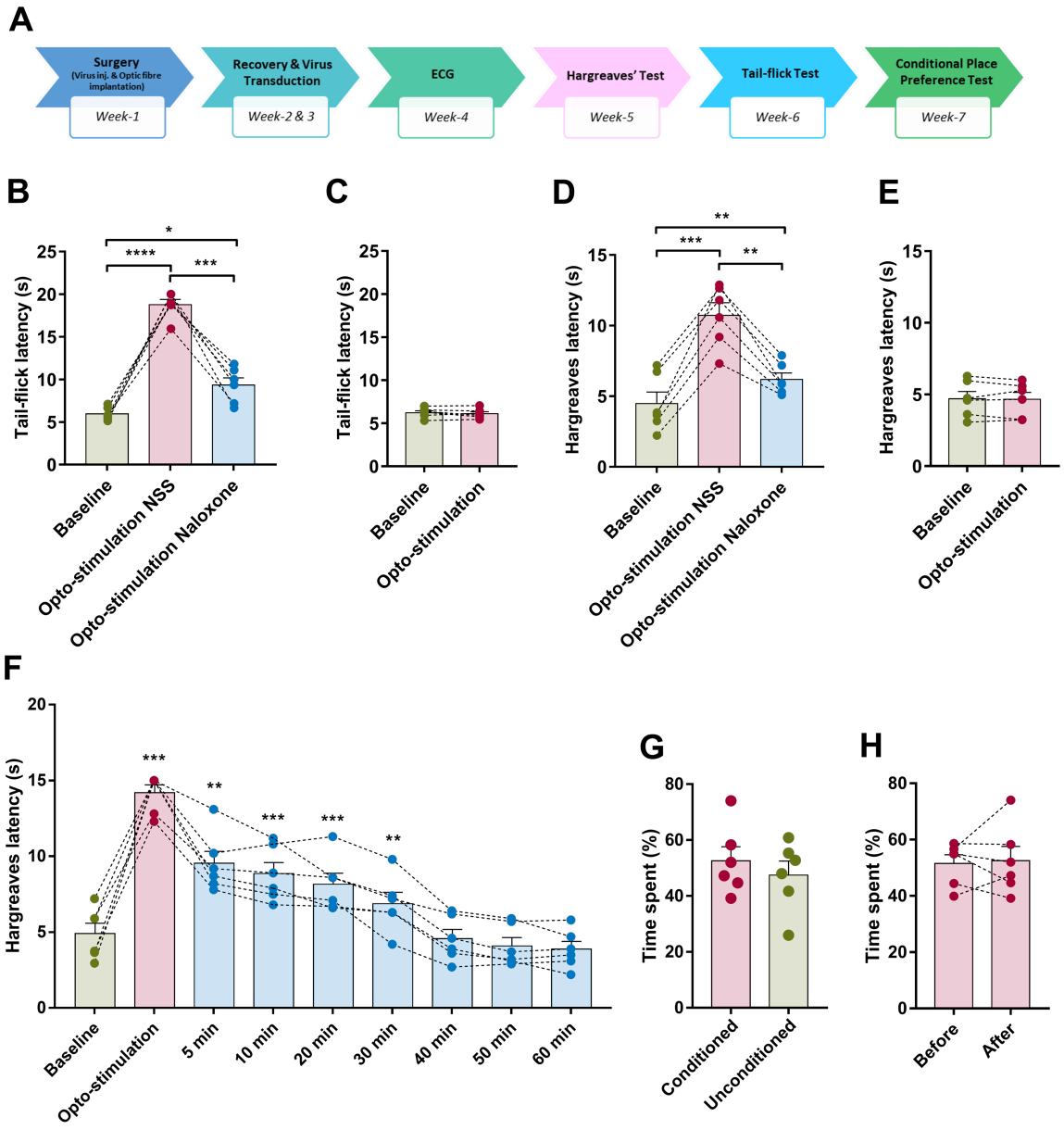
A
Surgery
(Virus inj. & Optic fibre implantation)
Week-1
Recovery & Virus Transduction
Week-2 & 3
ECG
Week-4
Hargreaves' Test
Week-5
Tail-flick Test
Week-6
Conditional Place Preference Test
Week-7
B
Tail-flick latency (s)
Baseline
Opto-stimulation NSS
Opto-stimulation Naloxone
C
Tail-flick latency (s)
Baseline
Opto-stimulation
D
Hargreaves latency (s)
Baseline
Opto-stimulation NSS
Opto-stimulation Naloxone
E
Hargreaves latency (s)
Baseline
Opto-stimulation
F
Hargreaves latency (s)
Baseline
Opto-stimulation
5 min
10 min
20 min
30 min
40 min
50 min
60 min
G
Time spent (%)
Conditioned
Unconditioned
H
Time spent (%)
Before
After

Figure 4

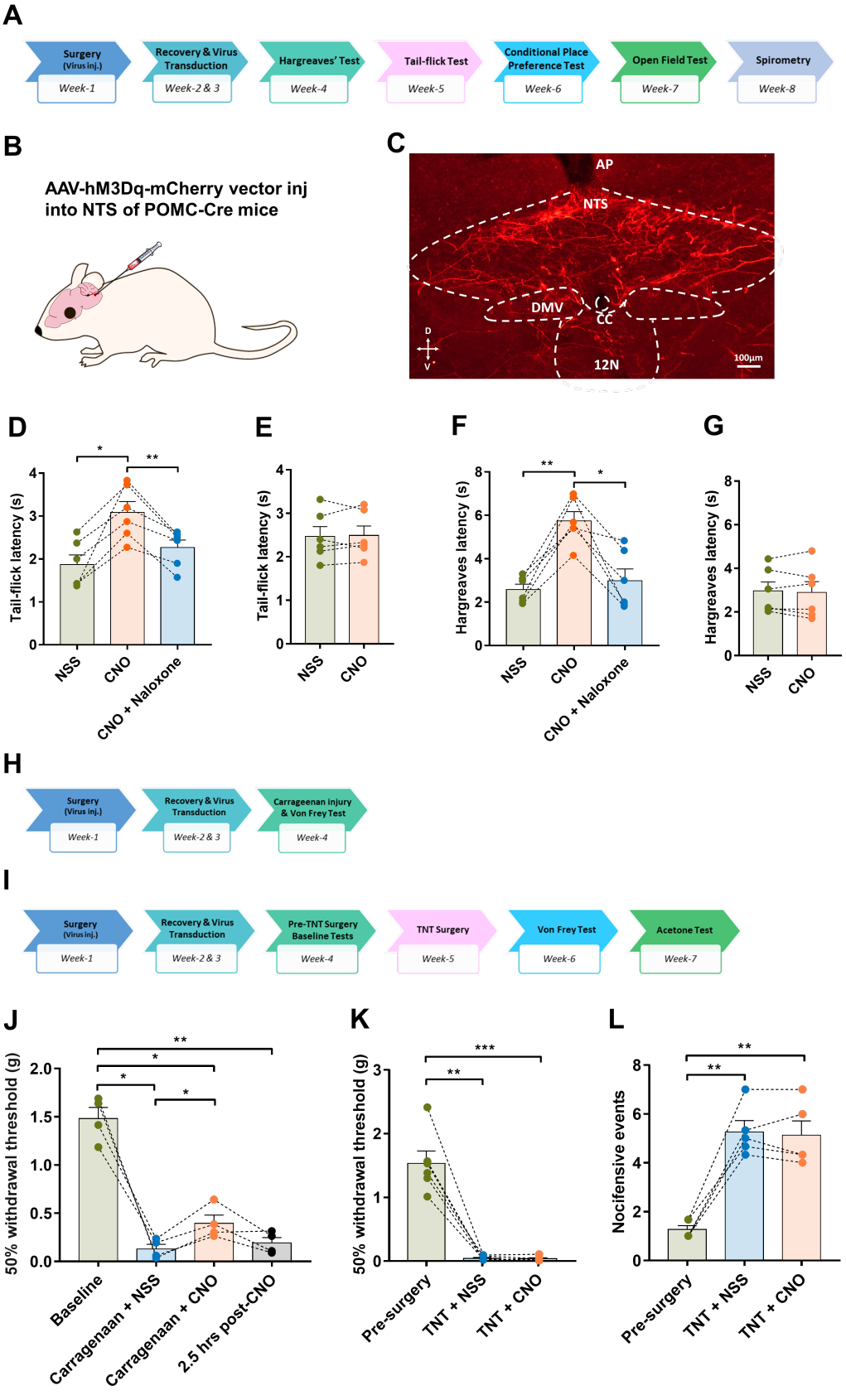
A
Surgery (Virus inj.)
Week-1
Recovery & Virus Transduction
Week-2 & 3
Hargreaves' Test
Week-4
Tail-flick Test
Week-5
Conditional Place Preference Test
Week-6
Open Field Test
Week-7
Spirometry
Week-8
B
AAV-hM3Dq-mCherry vector inj into NTS of POMC-Cre mice
C
AP
NTS
DMV
CC
12N
100µm
D
Tail-flick latency (s)
NSS
CNO
CNO + Naloxone
E
Tail-flick latency (s)
NSS
CNO
F
Hargreaves latency (s)
NSS
CNO
CNO + Naloxone
G
Hargreaves latency (s)
NSS
CNO
H
Surgery (Virus inj.)
Week-1
Recovery & Virus Transduction
Week-2 & 3
Carrageenan injury & Von Frey Test
Week-4
I
Surgery (Virus inj.)
Week-1
Recovery & Virus Transduction
Week-2 & 3
Pre-TNT Surgery Baseline Tests
Week-4
TNT Surgery
Week-5
Von Frey Test
Week-6
Acetone Test
Week-7
J
50% withdrawal threshold (g)
Baseline
Carragenaan + NSS
Carragenaan + CNO
2.5 hrs post-CNO
K
50% withdrawal threshold (g)
Pre-surgery
TNT + NSS
TNT + CNO
L
Nocifensive events
Pre-surgery
TNT + NSS
TNT + CNO

Figure 5

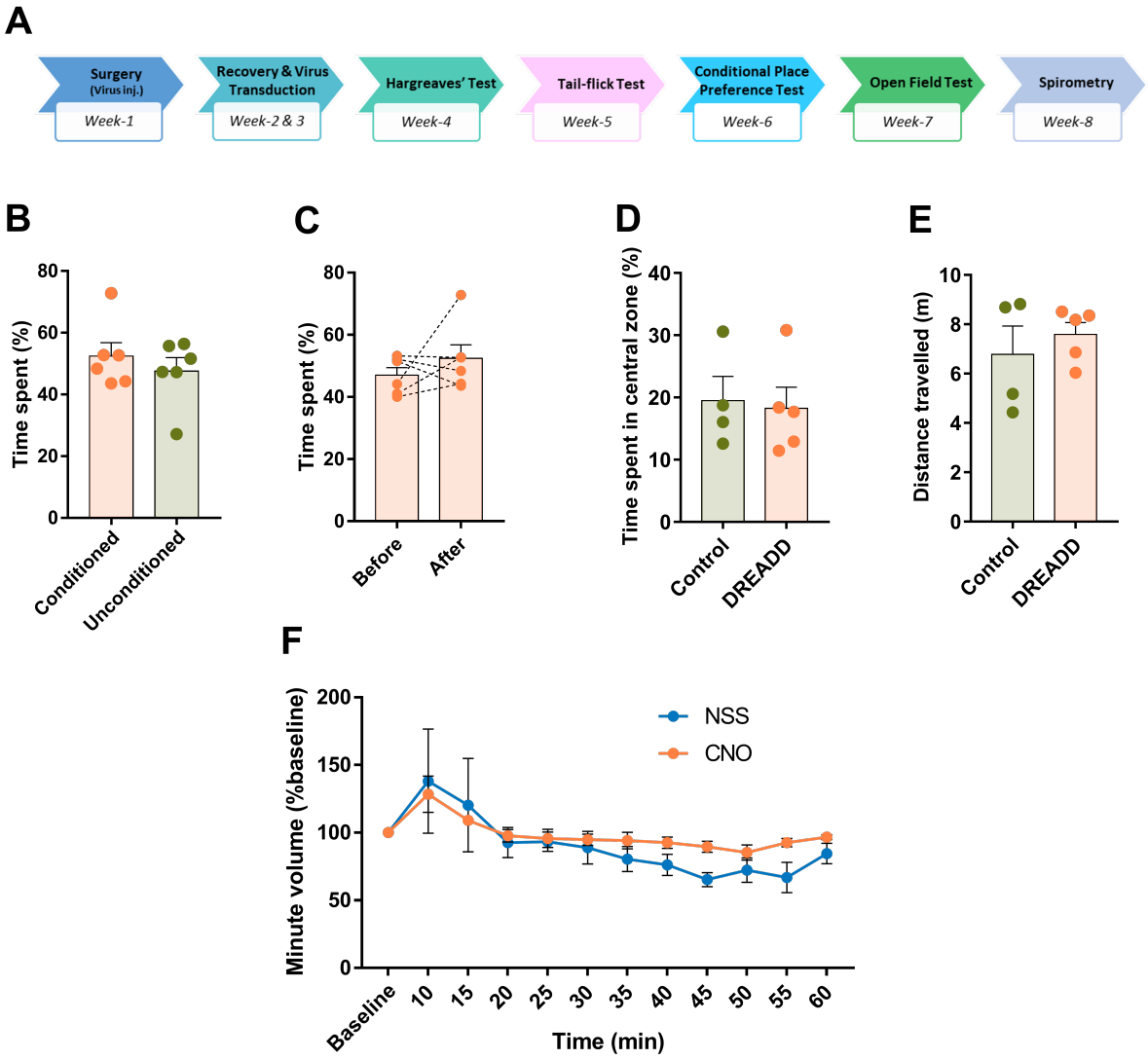
A
Surgery (Virus inj.)
Week-1
Recovery & Virus Transduction
Week-2 & 3
Hargreaves' Test
Week-4
Tail-flick Test
Week-5
Conditional Place Preference Test
Week-6
Open Field Test
Week-7
Spirometry
Week-8
B
Time spent (%)
Conditioned
Unconditioned
C
Time spent (%)
Before
After
D
Time spent in central zone (%)
Control
DREADD
E
Distance travelled (m)
Control
DREADD
F
Minute volume (%baseline)
NSS
CNO
Baseline
Time (min)

Figure 6

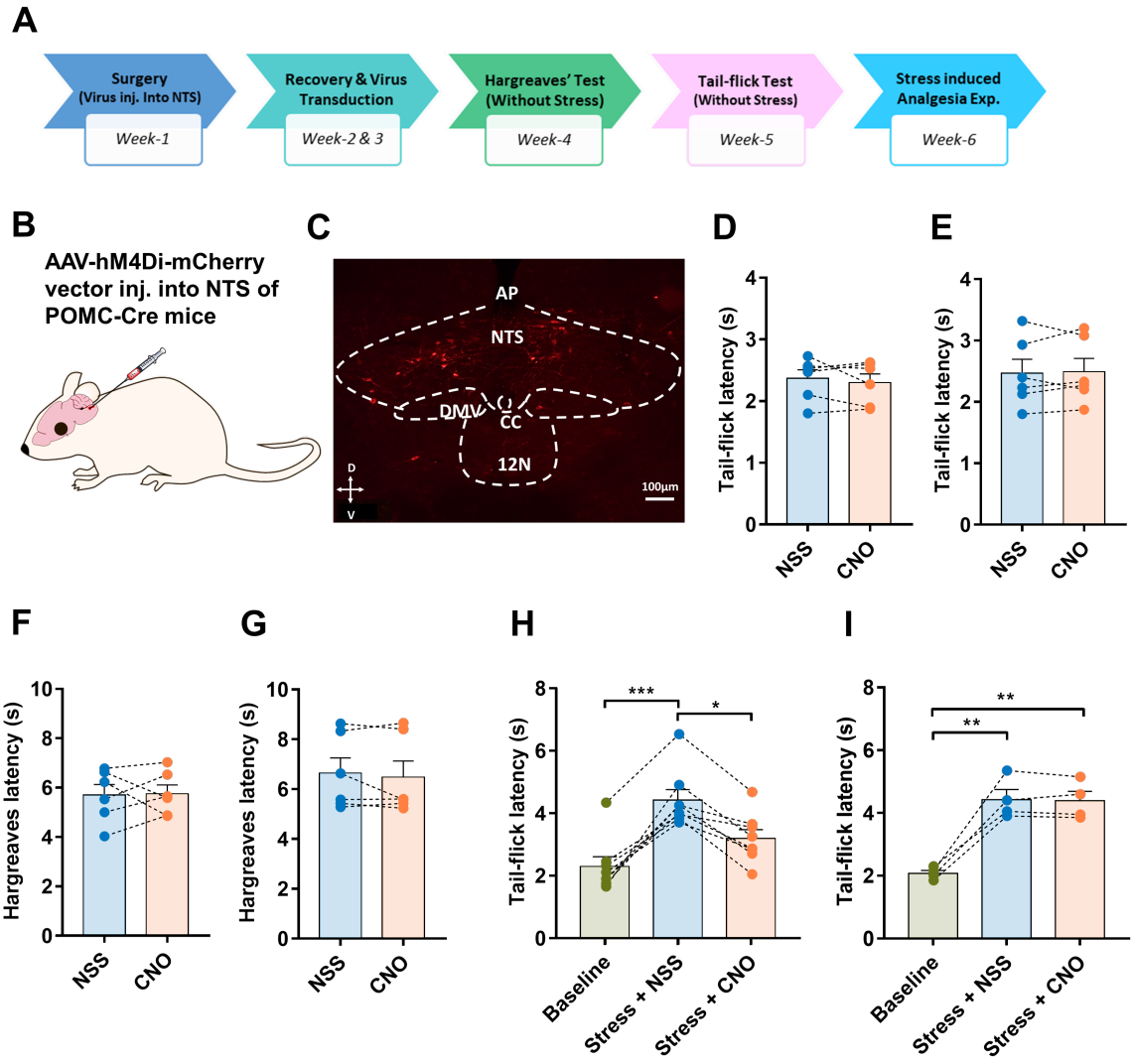
A
Surgery (Virus inj. Into NTS)
Week-1
Recovery & Virus Transduction
Week-2 & 3
Hargreaves' Test (Without Stress)
Week-4
Tail-flick Test (Without Stress)
Week-5
Stress induced Analgesia Exp.
Week-6
B
AAV-hM4Di-mCherry vector inj. into NTS of POMC-Cre mice
C
AP
NTS
DMV
CC
12N
100µm
D
E
Tail-flick latency (s)
NSS
CNO
F
Hargreaves latency (s)
G
H
Baseline
Stress + NSS
Stress + CNO
***
*
I
**